Next Generation Probabilistic Prediction Model for Submarine Propulsion Shaft Life

by

Daniel Duc Cong Huynh

B.S. Systems Engineering, United States Naval Academy (2006)

Submitted to the Department of Mechanical Engineering
in partial fulfillment of the requirements for the degrees of
Naval Engineer
and
Master of Science in Mechanical Engineering
at the
MASSACHUSETTS INSTITUTE OF TECHNOLOGY
June 2018

Author .....
Department of Mechanical Engineering
May 11, 2018

Certified by .....
Ronald G. Ballinger
Professor of Nuclear Science and Engineering
Professor of Materials Science and Engineering
Thesis Supervisor

Certified by .....
Alexander H. Slocum
Walter M. May and A. Hazel May Professor of Mechanical Engineering
Thesis Supervisor

Accepted by .....
Rohan Abeyaratne
Chairman, Committee on Graduate Theses
Department of Mechanical Engineering

Next Generation Probabilistic Prediction Model for Submarine Propulsion Shaft Life

by

Daniel Duc Cong Huynh

Submitted to the Department of Mechanical Engineering
on May 11, 2018, in partial fulfillment of the
requirements for the degrees of
Naval Engineer
and
Master of Science in Mechanical Engineering

Abstract

With the development of the U.S. Navy's new COLUMBIA class ballistic missile submarine, the Navy plans to implement a new, longer operational inspection interval for the propulsion shaft system, attempting to double the current 6-year inspection interval for the OHIO class of submarine it is replacing. However, an initial study conducted suggests unsatisfactory levels of failure at this interval due to corrosion fatigue, although with a high level of uncertainty. This thesis addresses that uncertainty by developing a more robust probabilistic model for submarine propulsion shaft reliability in order to more accurately predict probabilities of failure.

To improve upon previous efforts, all the components and failure modes of the propulsion shaft were first identified. While the most likely scenario involves water ingress and a wetted propulsion shaft leading to corrosion, pitting, and cracking, other factors that could contribute to shaft failure include damage during installation or failure of cathodic protection systems. Using literature and data gathered during visits to Portsmouth Naval Shipyard (PNSY), these failure modes were approximated with appropriate relationships and statistical distributions and ultimately combined to form a complete probabilistic model of the propulsion shaft system, including all the expected components and the best physics available. Additionally, while this model was designed with extension to the COLUMBIA class of submarine in mind, it can be tailored and easily modified to apply to a broad range of shafting systems, including other classes of submarines, conventional surface ships, and even offshore platforms.

The GoldSim program was used as the vehicle for the model, with failure probabilities for the submarine shaft predicted using Monte Carlo simulations. To calibrate the model, outputs from the probabilistic model were compared against hypothetical shaft inspection data, adjusting distributions and variables as appropriate to match target values. While the model used the OHIO class submarine as its baseline, it is expected that the new COLUMBIA class shafting system will use similar mate-

rials and have a similar configuration. These inspections have typically taken place at around the 6-year operational interval, but the calibrated model can be used to predict propulsion shaft failures at a range of inspection intervals.

Thesis Supervisor: Ronald G. Ballinger
Title: Professor of Nuclear Science and Engineering
Professor of Materials Science and Engineering

Thesis Supervisor: Alexander H. Slocum
Title: Walter M. May and A. Hazel May Professor of Mechanical Engineering

Acknowledgments

As I sit and reflect upon the conclusion of my time here at MIT, I'm reminded of the journey I've experienced these last few years and thankful to all the people who have supported and influenced me along the way.

To my advisors, Professor Ronald Ballinger and Professor Alex Slocum, I thank you for providing the guidance and leadership that I needed to complete my thesis this past year. The wealth of knowledge and experience that both of you possess was indispensable, and I look forward to hearing about the great innovations in propulsion shafting that your research will undoubtedly spearhead.

To Dr. Douglas Jonart, not only did you produce the framework from which I built my research, but your assistance from the very beginning, even from afar, was invaluable to ensuring I was consistently pointed in the right direction.

To my classmates and friends, no journey would be complete without you. From the karaoke bar to the tennis court, I am thankful for the encouragement and balance you all provided me.

And of course, I would like to thank my family. To my parents and my sister, you were my foundation that I could always rely on these last three years. Your contribution may not always be tangible, but the support you provided me never went unnoticed, and I sincerely thank you.

THIS PAGE INTENTIONALLY LEFT BLANK

Contents

List of Figures

List of Tables

THIS PAGE INTENTIONALLY LEFT BLANK

Chapter 1

Introduction

The total acquisition cost of the U.S. Navy's new COLUMBIA class ballistic missile submarine is projected to exceed $100 billion[1], with the lead ship estimated to cost over $8 billion[1] [1]. With the first in the class scheduled to be procured in FY2021, this platform will be constructed with the latest stealth technologies and fitted with the most advanced systems to ensure operability during its planned 42-year service life [1]. With all the innovative machinery onboard, one piece of equipment will at least be equally as important, if not more, to the safe operation of the submarine — the propulsion shaft system.

Shaft systems provide a very important role in most complex devices, transferring torque and power between often distant components that require relative motion [2]. Whether it is the drive shaft on an automobile or the propeller shaft on ships and submarines, ensuring the functionality and reliability of this system is paramount to the proper function of these machines. Many of these systems have remained relatively unchanged for years, and through proper design, engineering, and regular maintenance periodicities, most of these systems can be relied on to operate as expected for their entire service life. However, when one or more of the factors change, proper risk mitigation and analysis must be performed.

[1] In FY2017 dollars

Figure 1-1: OHIO Class Ballistic Missile Submarine (SSBN)[2]

1.1 Reliability and Risk Analysis

The current classes of U.S. Navy submarines, including the OHIO class that the COLUMBIA will be replacing, typically undergo a propulsion shaft inspection every 6 years with the purpose of finding and repairing imperfections and evidence of corrosion before they turn into cracks, which could result in a catastrophic failure. With the development of the COLUMBIA class, the Navy wants to move toward a longer inspection interval in order to reduce the number and length of maintenance overhauls and increase overall availability [3].

To determine the feasibility of this change, a proper risk analysis must be performed. One such method involves a Failure Mode and Effects Analysis (FMEA), where all the various failure modes of the system are identified along with their respective effects. By modeling these failure modes probabilistically, estimated probabilities of failure can be determined. These estimated failure probabilities can subsequently be used to determine appropriate inspection intervals for the system, properly miti-

[2]This image is of the OHIO class ballistic missile submarine USS KENTUCKY near Puget Sound, Washington, taken on March 13, 2016 by Mass Communication Specialist 2nd Class Amanda R. Gray. The photo was released as public domain and can be accessed at http://www.csp.navy.mil/Media/News-Articles/Display-News/Article/693364/kentucky-departs-for-first-strategic-mission-since-2011/.

gating the risk. For these new classes of submarines, while determining the viability of a 12-year inspection interval is the primary goal, an ultimate objective is to develop a propulsion shaft system where the required inspection interval exceeds the service life of the vessel, eliminating the need for inspections altogether. Since the shaft inspections require an extended dry-docking, eliminating them would represent a significant increase in availability. The U.S. Navy has had success with similar tasks in the past, with recent classes of submarines possessing a life-of-the-ship nuclear fuel core [1].

The benefit of probabilistic models over traditional deterministic models is that the former can incorporate randomness and uncertainty in the estimated outcome — in this case time to failure. This is often done using Monte Carlo simulation, where a model is run a large number of times with probabilistic inputs (uncertainty distributions) in order to determine a distribution of the possible outcomes. For this model, the elements that factor into the service life of the propulsion shaft are affected by variations and unpredictability in multiple phenomena, including material properties, loading history, environmental conditions, and corrosion morphology (pit, crack geometry), making a probabilistic-based approach more appropriate for the prediction of damage [4]. To model the propulsion shaft system and perform the Monte Carlo simulations in this thesis, the program GoldSim is used. The process is described in more detail in Chapters 3 and 4. More information on GoldSim can be found in Appendix A.

1.2 Approach

An initial study to estimate the effect of uncertainty on the desired increase in the inspection interval yielded unsatisfactory levels of failure due to corrosion fatigue[3], albeit with several simplifications and a high level of variability [6]. The goal of

[3]Corrosion fatigue is defined as the process leading to failure due to cyclic or alternating stresses in a corrosive environment. It is considered the main failure mechanism for structures such as rotating shafts in seawater that undergo cyclic stresses [5]. Corrosion fatigue is described in more detail in Chapter 2.

this thesis is to develop a more robust, probabilistic model of the propulsion shaft system on a COLUMBIA-like class of submarine in order to better characterize the effect of that uncertainty and more accurately estimate whether increasing the shaft inspection interval will result in unacceptable failure rates. A key attribute of the model is the inclusion of all the relevant physics and engineering features. Due to classification, model calibration is done using representative target values based on hypothetical inspection results from OHIO class submarines, since it is expected that the COLUMBIA class will have a similar design. However, the model can quickly be calibrated to real-world data points by using actual shaft inspection results, improving accuracy and applicability.

While the model in this thesis focuses on open-sourced information regarding submarines and the COLUMBIA class specifically, it can be easily modified to model a wide range of shafting systems, including surface ships, automobiles, and even offshore platforms, given that the components and appropriate statistical distributions are known or can be determined.

The method to develop this updated probabilistic model followed these general steps.

1. Review existing literature and research in order to determine areas for improvement and uncertainty reduction.

2. Use Monte Carlo simulation software (GoldSim) to model and recreate the initial simplified shaft model in order to validate relationships and statistical distributions.

3. Incorporate additional shaft components and failure modes.

4. Reassess assumptions and recalibrate random variables using literature and simulation target values.

5. Determine new failure probabilities at a range of inspection intervals with recommendations for future work.

1.3 Overview

Chapter two provides background information on submarine shafting systems and their typical failure modes. The existing propulsion shaft model and the general corrosion fatigue chain utilized are also examined, along with areas for improvement.

Chapter three describes the current study for improving the shaft life prediction model, including additional corrosion considerations such as galvanic corrosion, cathodic protection, and coatings. Model assumptions are discussed, followed by a description of the next-generation probabilistic propulsion shaft model, complete with the updated corrosion fatigue process that forms its basis. The description includes how the prediction model applies the new corrosion fatigue steps to common submarine shaft components. The chapter concludes with an illustration of how the model is created within GoldSim.

The Monte Carlo parameters, target values, and simulation results are discussed in Chapter four. Using the results, a prediction for the propulsion shaft life of a COLUMBIA-like submarine is made, along with an examination of the feasibility of a 12-year inspection interval. A sensitivity analysis, model limitations, and a discussion of the associated uncertainty complete the chapter.

Finally, Chapter five provides conclusions and recommendations for future work, including methods to improve future iterations of the model based on tailored experiments and data availability.

Appendix A provides a brief overview of the GoldSim program, and Appendix B lists abbreviations and symbols used in this thesis.

THIS PAGE INTENTIONALLY LEFT BLANK

Chapter 2

Prevailing Discussions and Models

This chapter provides contextual information on the construction and operation of submarine propulsion shafts followed by a review of the existing shaft life prediction model and the corrosion fatigue process it incorporates. The concepts discussed rely heavily on the previous work by Jonart [6], who developed the original propulsion shaft model. A discussion on potential areas for model improvement concludes the chapter.

2.1 Naval Context

A simplified diagram of a typical Naval submarine propulsion shaft is shown in Figure 2-1, with the submarine's aft end on the left side of the image. Some fundamental components are labeled, including the stern tube and propeller bearings, along with potential areas of concern for corrosion fatigue due to material, geometry, and loading. Not marked is a glass-reinforced plastic (GRP) coating that encases the steel shaft in all areas between the two bearings.

To obtain a better understanding of the shaft life problem, it is beneficial to understand the basic operation of the system. The submarine's main engines, which are not pictured, rotate the shaft and propeller. Differential pressure created at the propeller produces a force which is transferred along the shaft to the thrust block, which is structurally connected to the hull. The thrust block resists the axial force,

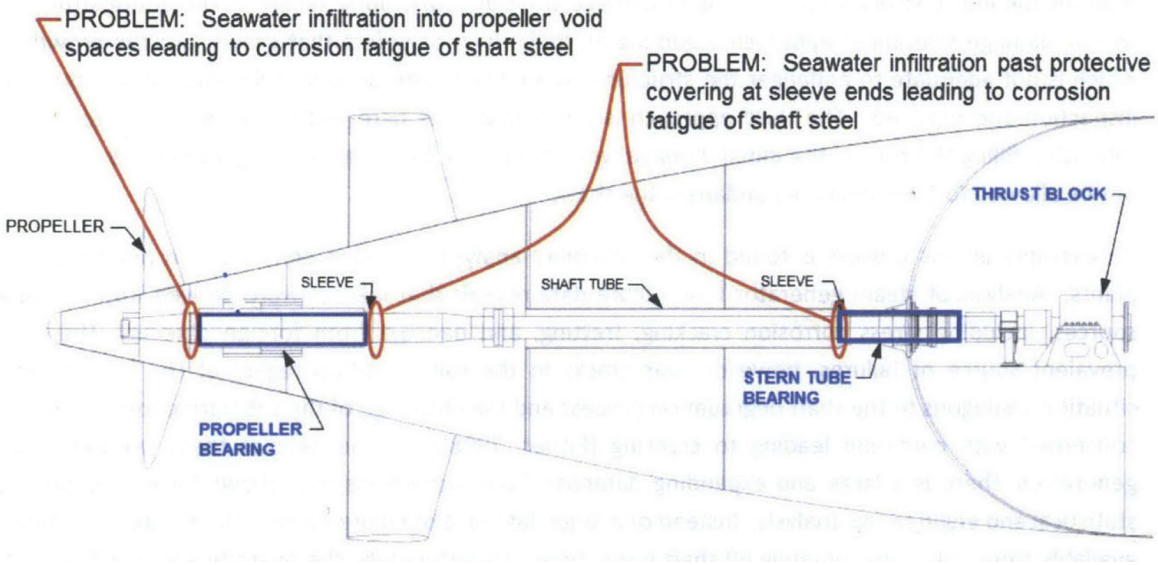

Figure 2-1: Simplified Submarine Shaft Diagram[1]

propelling the submarine forward. The shaft itself is supported by bearings and in the case of a submarine, has to penetrate a watertight pressure boundary, represented by the semicircle on the right side of the diagram. The load on the shaft is dependent on many factors, including the drag resistance of the hull to the power and torque output of the engines. A more detailed discussion of some of these components and how they fit into the probabilistic model is given in Chapter 3.

Developing a model for such a large and complex system is challenging, especially given the scarcity of open-sourced literature on submarine construction and operation. For the propulsion shaft specifically, not only does it experience torsional, shear, and axial forces, but also large bending moments due to the weight of the propeller [7]. Consequently, it is usually constructed from a high strength metal, such as a mild/carbon steel. With the presence of a strong electrolyte such as seawater, the potential for corrosion fatigue is high if access to the steel is gained.

While most shaft failures typically have damaging consequences, the failure of a submarine propulsion shaft would be catastrophic. As Figure 2-1 illustrates, most modern submarines only possess one shaft, meaning a single failure would cripple

[1]Figures 2-1 and 2-5 were originally presented at Shaft Life Advancement Industry Day at the Massachusetts Institute of Technology on October 13, 2011. They were used in the doctoral dissertation by Douglas Jonart (MIT), Reference [6], and are reprinted with permission.

the entire propulsion system. Unlike shaft systems on land or on floating platforms, failure on a submerged submarine could also cause uncontrolled flooding, risking loss of the whole vessel.

For the purposes of this thesis, shaft failure is defined as a circumferential crack that propagates around the complete perimeter. While failures could result from a variety of sources, such as a material degradation or a mechanical failure due to a large external force (such as in a collision), the most prevalent and concerning issue is from corrosion fatigue [5]. Thus, this thesis will focus on this mode of failure, recognizing that other means of failure are uncommon and unlikely.

2.2 Corrosion Background

In its simplest definition, corrosion is the "degradation of a material through environmental interaction" [8]. The corroding material loses electrons through an oxidation reaction, also called an anodic reaction, such as the iron reaction seen in Equation (2.1). These electrons are consumed through a reduction reaction (cathodic reaction), as seen in Equations (2.2) and (2.3) [8, 9].

$$Fe \rightarrow Fe^{++} + 2e^{-} \tag{2.1}$$

$$O_2 + 2H_2O + 4e^{-} \rightarrow 4OH^{-} \tag{2.2}$$

$$2H_2O + 2e^{-} \rightarrow H_2 + 2OH^{-} \tag{2.3}$$

The mechanism for corrosion can take on a variety of forms with vastly different effects. Crevice corrosion, for example, generally occurs in small gaps or grooves where the local chemistry can be immensely different from that of the bulk fluid [9, 10]. Pitting corrosion, on the other hand, occurs at passive film disruptions, mostly on stainless steels and aluminum alloys [9, 10, 11]. While each of these corrosion types may be present in mild steel shaft material exposed to seawater, the primary mechanism for corrosion (pH $=\sim 7$) is uniform corrosion, commonly called general

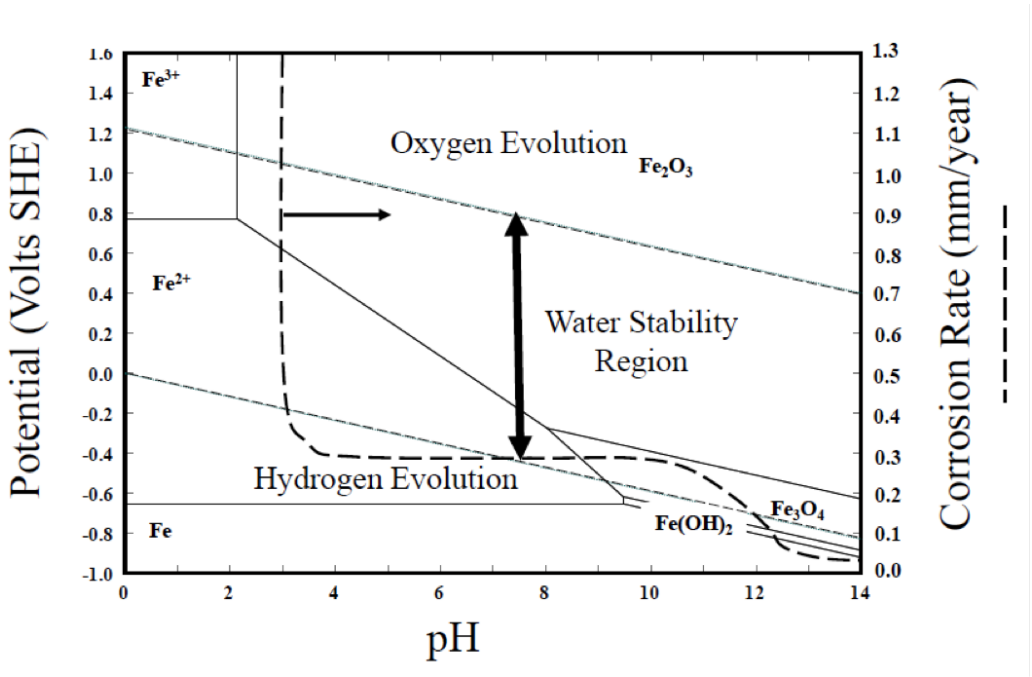

Figure 2-2: Stability Diagram for Iron in Water with Approximate Corrosion Rates Superimposed [12]

corrosion, which results in a relatively even loss of material where the oxide film is stable. The material loss is usually defined by an average depth of penetration calculated from weight loss measurements [11].

To illustrate these different mechanisms, Figure 2-2 shows a plot of potential (effectively "energy") vs. pH (hydrogen ion concentration) for the iron-water system, frequently called a stability, or Pourbaix, diagram. Also shown (right axis) is the approximate corrosion rate for iron in aerated water. Two items of note are the effect of the presence of a stable oxide film ("passivity") on the corrosion rate and the significant increase in corrosion rate where the iron ions are stable. While general corrosion is usually the result, in cases where the pH is reduced with stable iron ions, such as in pitted or creviced conditions, the corrosion rate can be very high. In such cases, it is possible for a separated anode and cathode situation to develop, resulting in greatly accelerated corrosion in the anodic region. This would be the situation for pitting or crevice corrosion [12].

However, though the name "general corrosion" seems to imply otherwise, there are cases where small surface depressions can result from uneven uniform corrosion,

eventually leading to the formation of pit-like features. As Jonart has discussed, it is important to differentiate between these corrosion pits that form during uniform corrosion and the previously mentioned pitting corrosion, especially since much of the literature regarding pit nucleation and growth has been focused on the latter [6]. The key differences between the pit-like development that can occur in iron alloys and true pitting corrosion have to do with the degree of stress concentration and the local chemistry changes that can occur. True pits have a very high aspect ratio (depth/width), which results in stress concentration factors of 3 or more. The aspect ratio for pit-like features in iron alloys in seawater is usually no higher than 2 — creating a much smaller stress concentration [12]. Also, higher aspect ratio pits facilitate the development of localized chemistry and pH depression, which can shift the pH to a higher corrosion rate region. However, to further complicate the situation, the presence of a galvanic couple (steel coupled to a nickel-based alloy for example) can also accelerate the local corrosion rate of the steel with only a gradual increase in aspect ratio, and hence, stress concentration [12]. Galvanic couples are discussed more in the next chapter.

One popular general corrosion model is the nonlinear framework developed by Melchers, with Figure 2-3 obtained from his model [11]. In it, he discusses five distinct corrosion phases (numbered 0 to 4), with each phase being controlled by a different mechanism and resulting in a different corrosion loss rate [13].

While Melchers' research is widely accepted, its main application is for plating and structural capacity analysis, not corrosion fatigue life determination, which is the dominant mechanism that influences submarine shaft life prediction [5]. Thus, additional literature needed to be examined.

2.3 Corrosion Fatigue Model

As it happens, extensive literature exists regarding corrosion fatigue of carbon steel in a seawater environment. One example is Li and Akid's corrosion fatigue model for carbon steel shaft material in seawater, with emphasis on pit development on

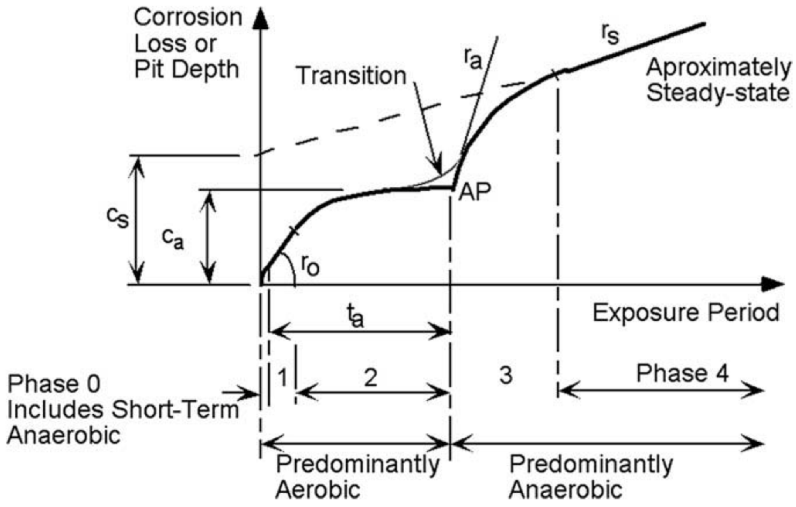

Figure 2-3: Melchers' Mild Steel General Corrosion Model[2]

initially defect-free surfaces [5]. Pérez-Mora, Palin-Luc, Bathias, and Paris similarly investigated the effects of a corrosive seawater environment on carbon steel, focusing more in the very high cycle fatigue regime [14]. Arzaghi et al. and Goto investigated corrosion fatigue behavior of subsea high strength steel pipelines and heat-treated carbon steel, respectively [15, 16].

Additional literature also exists for probabilistic modeling of the corrosion fatigue process. Harlow and Wei, who looked predominantly at aluminum alloys, and the aforementioned Melchers have each published numerous articles discussing probabilistic modeling, some of which formed the backbone of the previous COLUMBIA-like shaft life model developed by Jonart [11, 13, 17].

2.3.1 Application to Shaft Life

The previous submarine propulsion shaft model was essentially a corrosion fatigue model that followed six general phases in the degradation process: water ingress, corrosion, pitting, pit-to-crack transition, crack growth, and failure, as illustrated in Figure 2-4 [6]. Most of the phenomenology of the corrosion model came from the work

[2]This diagram was taken from Gudze and Melchers "Operational based corrosion analysis in naval ships" [18, p. 3298], but is based on Melchers' marine immersion corrosion model seen in many of his individual works [11, 13].

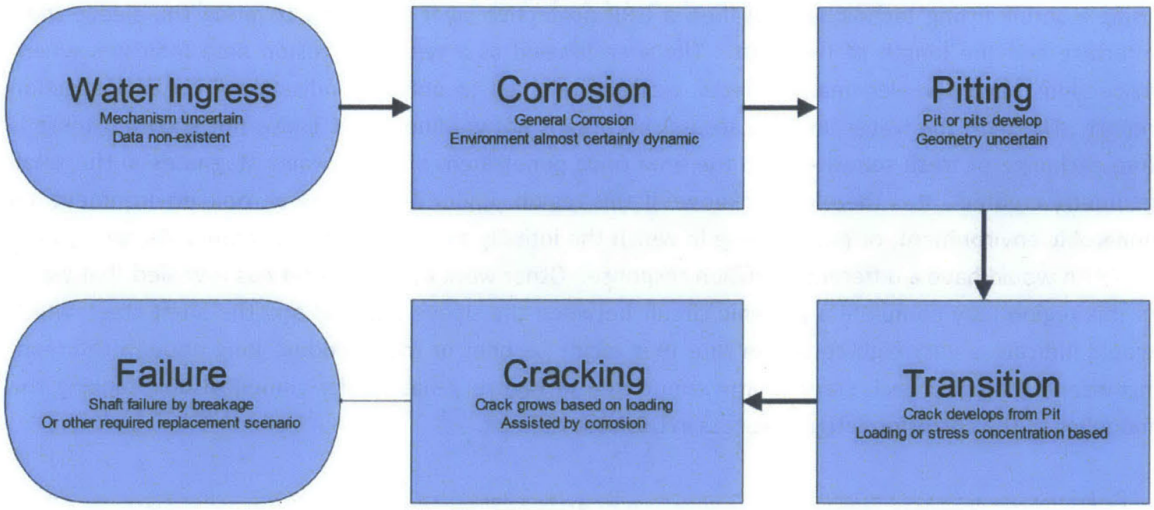

Figure 2-4: Six-Stage Corrosion Fatigue Model[3]

of Shi and Mahadevan, who built upon the research of Harlow and Wei and others to develop a seven-stage corrosion fatigue framework that starts at pit nucleation and ends with short and long crack propagation [19]. The addition of the water ingress stage was needed to describe the time required for seawater to penetrate the coatings and seals around the shaft and access the mild steel itself.

By probabilistically applying the major stages of this corrosion process to a submarine propulsion shaft, the fatigue life can be modeled and predicted, after assuming a time to water ingress distribution. However, while the process of corrosion fatigue has been thoroughly researched and reviewed, its application to submarine shafts involves extensive simplifications and assumptions.

2.3.2 Areas for Improvement

The original model predicted that a propulsion shaft design similar to the OHIO class submarine will experience a 45% mean failure probability when assuming a 12-year inspection interval. This value was based on probabilistically extrapolating the 6-year inspection data points through application of corrosion fatigue principles [6]. While water ingress prevention represents the best way to preclude these corrosion fatigue

[3]This diagram was taken from the doctoral dissertation by Douglas Jonart (MIT), Reference [6], and is reprinted with permission.

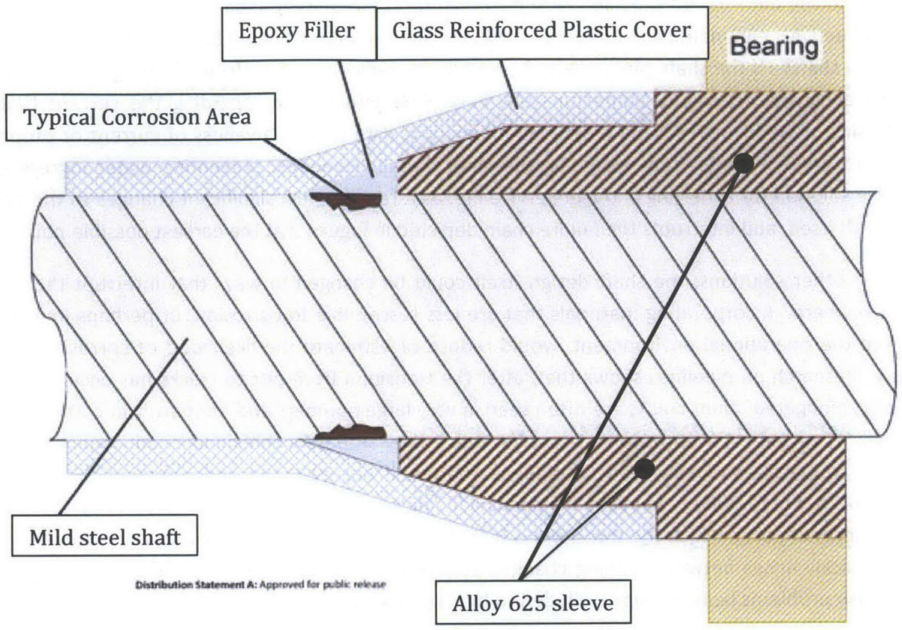

Figure 2-5: Shaft to Bearing Sleeve Interface Diagram[1,4]

failures, model improvements could also shed light on other prevention methods, as well as provide more representative results and estimations of uncertainty.

The existing model assumed the shaft acted as one complete entity, a significant simplification since each of the various components seen in Figure 2-1 undergo distinct corrosion processes due to varying composition, geometry, and loading. The two bearings, seen in more detail in Figure 2-5, are prime examples because the interface between the mild steel shaft and the Alloy 625[4] bearing sleeve creates potential for a galvanic couple that can greatly accelerate corrosion of the less noble material, which in this case is the shaft [21]. A more detailed discussion of galvanic corrosion is presented in Section 3.1.1, with how it is incorporated in the updated propulsion shaft model in Section 3.3.

Additionally, the earlier shaft life model only accounted for one water ingress method, which Jonart modeled using a highly skewed Weibull distribution [6]. How-

[4]Alloy 625 is a nickel-chromium alloy that is part of the Inconel family trademarked by the Special Metals Corporation group of companies. Known for its high strength and excellent corrosion resistance, the alloy is frequently used in seawater applications such as the propeller blades on motor patrol gunboats and the auxiliary propulsion motors on submarines, in addition to the bearing sleeves seen here [20].

ever, in addition to straightforward seawater permeation through the shaft coating, water ingress time is also impacted by flaws and damage to the coating surface, known as holidays[5], which could be caused by defects or during installation and have a substantial effect on corrosion fatigue life. Jonart acknowledged this fact when suggesting that a compound distribution might better capture how some shafts experience coating failures very early in their service life [6].

For the pitting phase specifically, areas for improvement include accounting for temperature variations due to submarine operating depth, loading disparities between different components, and adjusting for the presence of cathodic protection. Furthermore, most of the corrosion fatigue tests in literature model crack growth using the stress intensity factor of an infinite plate. Modifying it to account for a cylindrical shaft geometry would improve the model and produce more realistic shaft life predictions.

As an early attempt at modeling shaft life on a submarine class that has not even been fully designed yet, there are obviously many more areas where the original prediction framework can be improved, with Chapter 3 discussing the areas that were incorporated into the next-generation probabilistic model.

[5]In corrosion control, a holiday is a term used to describe a hole or discontinuity in the coating surface.

THIS PAGE INTENTIONALLY LEFT BLANK

Chapter 3

Current Research

The mechanism of corrosion fatigue is complicated and dependent on a multitude of variables [9, 13, 18]. However, given the complexity of a billion-dollar submarine where shaft reliability is a key requirement of the design, the value of developing a robust shaft life prediction model becomes evident. This chapter discusses possible areas to improve upon the existing corrosion fatigue framework along with methods to incorporate them into the next-generation probabilistic model.

Organizationally, the chapter commences with a discussion of additional corrosion considerations before examining model assumptions and ultimately, the probabilistic shaft life model itself. One important feature to note is that this next-generation model depicts each shaft component separately, complete with its own unique sub-model — including unique variables and statistical distributions that feed into a distinct corrosion fatigue process. As a result, each component has its own corrosion fatigue life. Failure of the shaft system, consequently, occurs when any of the individual components fail.

To aid in the explanation, the shaft model description is divided by corrosion fatigue segments, since each shaft component experiences the same general sequence of steps leading to failure. Within each segment, a description of the equations, variables, and distributions used to describe the degradation of each component can be found, to include major deviations from the original shaft model developed by Jonart. Concluding the chapter is an overview of how the model was implemented

using the GoldSim platform, with simulation results presented in Chapter 4.

3.1 Additional Corrosion Considerations

While the concepts of uniform corrosion and corrosion fatigue life were examined in Chapter 2, three additional corrosion considerations that play an important role in both concepts are galvanic corrosion, cathodic protection, and coatings.

3.1.1 Galvanic Corrosion

Galvanic corrosion, also called bimetallic corrosion, is a form of differential cell corrosion where the potential difference comes from two different metals electrically coupled and exposed in a conductive electrolyte [8]. The metal with the more positive potential becomes cathodically polarized while the more negative potential becomes anodically polarized. The cathode in the couple experiences reduced corrosion rates while the anode experiences accelerated corrosion rates [21].

One way to determine a metal's potential in a specific environment is to look at a galvanic series, similar to the simplified version shown in Figure 3-1. Based on the relative positioning of mild steel and nickel-chromium alloys such as Alloy 625 on the series, it is evident why galvanic corrosion is a concern for submarine shafting systems. As discussed earlier, the major components of the shafting system include a carbon steel shaft onto which an Alloy 625 sleeve bearing race is shrunk-fit. This combination creates a galvanic couple in which the carbon steel is the anode. To further aggravate the situation, the area of the Alloy 625 cathode is many times the size of the localized area of exposed carbon steel, should the interface between the shaft coating and the carbon steel/Alloy 625 region be breached. It is important to note that the galvanic series does not provide insight into corrosion rates, only corrosion potentials [9].

Rates of galvanic attack depend on corrosion current density, as seen in Equation (3.1) [22],

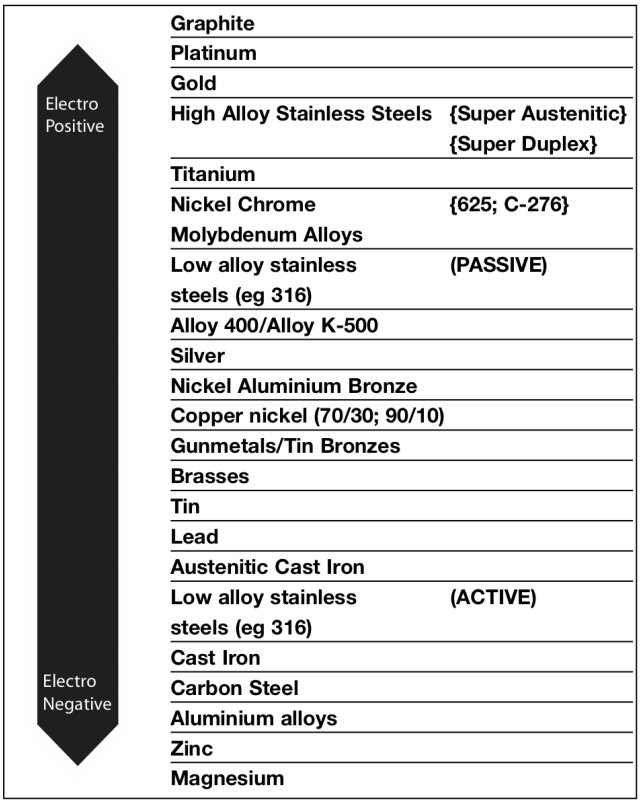

Figure 3-1: Simplified Galvanic Series Chart in Seawater[1]

$$Corrosion\ rate\ (mm/yr) = \frac{3.16 \times 10^8 \times i_{corr} \times M}{z \times F \times \rho} \tag{3.1}$$

where i_{corr} is the corrosion current density, M is the molar mass of the metal, z is the number of electrons transferred per metal atom (also known as valence), F is Faraday's Constant, and ρ is the density of the metal.

Equation (3.1) is a specific application of Kondo's volumetric corrosion equation based on Faraday's Law that is discussed in more detail in Section 3.3 [9, 23]. For mild steel in seawater, Kim et al. found current density to be 0.94 and 1.22 mA/cm^2 for natural seawater and NaCl solution (18.5 g/L), respectively [24]. Of course, the presence of galvanic couples will alter these values, depending on the materials involved.

[1]This figure was taken from the Bimetallic Corrosion Guide published by the National Physical Laboratory (NPL) in the United Kingdom [21]. Reprinted courtesy of NPL.

Perhaps the best way to prevent galvanic corrosion is to use the same material throughout the design, or at least materials with similar galvanic potentials. When that is not possible, cathodic protection measures and coatings may be considered [8], which are discussed next.

3.1.2 Cathodic Protection

Cathodic Protection (CP) works by making the metal that needs to be protected the cathode in an electrochemical cell, either with an impressed current or using a more active galvanic anode [8, 25].

For galvanic anodes, a more active metal, like zinc, is placed in electrical contact with the metal to be protected, a submarine shaft or hull for example. The more active metal drives the potential of the less active metal (iron in this case) in the cathodic direction. The shift of the potential in the negative direction reduces the corrosion rate of the iron. For this reason, galvanic anodes are often called sacrificial anodes, since they are sacrificed in place of the metal being protected. However, they have the limitation in that they can only supply a finite amount of current, which is typically low [8, 9].

For impressed current cathodic protection (ICCP) systems, the same current supplied by the galvanic anode is instead supplied by a power source. ICCP systems do not have the same current limitations as active metal anodes, but they pose a greater risk for overprotection issues. One such issue is stray current corrosion, where the excess current actually leads to corrosion of neighboring structures through interference [8]. Other problems include hydrogen embrittlement from excessive hydrogen generation [22] and cathodic shielding, which is more of a concern on systems with coatings, which is discussed more in Section 3.1.3 [26].

To prevent these concerns and determine the correct amount of protection current to supply, a reference electrode is commonly used to provide a "baseline" potential for control purposes. With CP applied, by measuring the potential between a metal and a reference electrode, an assessment of the level of protection can be obtained. A common criterion for steel structures in soil or water is to maintain a -850 mV

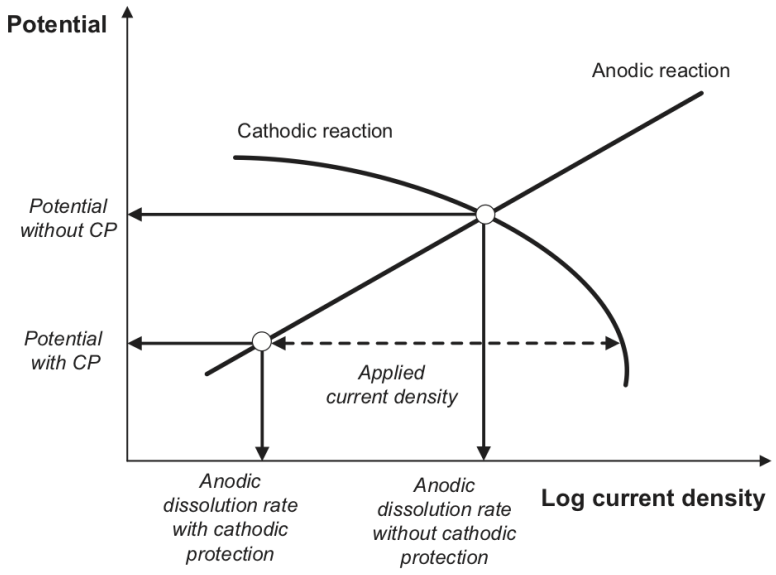

Figure 3-2: Evans Diagram Depicting Shifting Potential and Current Density due to Cathodic Protection [22]

potential versus a copper-copper-sulfate (CSE) reference electrode [8, 25]. At this potential, the corrosion rate of the steel is reduced to a minimum while avoiding the generation of hydrogen, which is an embrittling agent for high-strength steels.

With the proper CP current applied, estimating where the equilibrium potential and necessary current density for protection lies is usually done visually using an Evans[2] diagram, which plots the potential vs. current density. A schematic Evans diagram showing the effect of CP is shown in Figure 3-2. These plots for the cathodic (in most cases either oxygen or hydrogen reduction) and anodic reactions, known as polarization curves, are based on experimental measurements which often follow a linear relationship between the log of the current and the potential, known as Tafel behavior, with the slope of the curve commonly called the Tafel slope [22]. This linearity is often the case for the anodic reaction. However, as Figure 3-2 illustrates, this is not often the case for the cathodic reaction. The cathodic reaction is often controlled by mass transfer processes that are diffusion controlled. Thus, as the

[2]An Evans diagram is a mixed potential plot that depicts the relationship between the thermodynamics and kinetics of a corrosion process. The vertical axis is typically potential while the horizontal axis depicts current or current density [8].

current density increases, nonlinearity is observed with an eventual upper limit on the effectiveness of the cathode system [12].

3.1.3 Coatings

Another popular method to protect against corrosion, and hence corrosion fatigue, is with coatings. In theory, coatings are used to insulate the metal from the electrolyte and prevent the electrochemical reactions from taking place. However, due to the presence of flaws and imperfections inherent to all coatings, the main purpose ends up being to reduce the surface area exposed to the electrolyte and thus reduce the required current needed for cathodic protection [8].

While this is a significant advantage, depending on the condition of the coating, the required current can vary considerably. Apply too much current and the coating can become damaged and actually lose adhesion to the metal due to gas generation, creating crevices under the coating in a phenomenon called cathodic disbondment [8, 26]. The CP current cannot penetrate into these crevices, known as cathodic shielding, and localized corrosion can occur [26]. If the CP current is increased too much, excessive hydrogen will be produced due to water reduction, actually exacerbating the effect of cathodic shielding [26]. This occurrence poses more of a problem with ICCP systems but could also apply to galvanic anodes that are very active. In either case, research has proven that applying excessive CP current can actually reduce fatigue life, due most likely to hydrogen effects [27].

Furthermore, CP and coatings are not 100% effective and reliable. According to Melchers, the use of coatings, sacrificial anodes, and ICCP is extensive in practice, yet much evidence points to the fact that these systems are not always effective, especially "over longer time horizons and under less than ideal operational or maintenance conditions" [13]. Even with extensive research, it is hard to account for the complex environment and exact operational conditions experienced by the material, especially in empirical studies. Additionally, the influence of nearby AC currents can affect the corrosion rate and required protection currents [24]. As such, the NACE[3] Stan-

[3]NACE International is a professional organization founded as the National Association of Corro-

dard Practice does not assume that complete protection will be achieved, mentioning that CP is "a technique to reduce the corrosion of a metal surface," not necessarily eliminate it [25, 28].

3.1.4 Other Considerations

While galvanic couples and CP systems have a large and direct effect on corrosion current and current density, many other factors play a role in determining corrosion rates and corrosion fatigue life. The presence of calcareous deposits and oxide films on the metal surface can affect the anodic Tafel slope of the Evans diagram, affecting CP effectiveness [22]. Additional factors like salinity, oxygen concentration, pH, pollutants, temperature, pressure, bacteria, and surface roughness can also all affect corrosion rate [9, 13, 18].

For marine applications and especially for submarines, the effect due to temperature can vary based on operating area and depth. Melchers' experiments have shown that higher seawater temperatures generally lead to higher corrosion loss [11]. Temperature also affects dissolved oxygen levels, though factors such as pressure, salinity, and pollution levels can contribute [13]. Additionally, higher flow velocities can accelerate corrosion [13, 22], and more specifically to shaft systems, the rotation of the shaft itself can have an effect on CP [29].

3.2 Model Assumptions

With all the factors and circumstances that can influence corrosion current and corrosion fatigue life, in order to develop a shaft life prediction model, several assumptions need to be made. First and foremost, the model assumes only one failure mode, which is crack propagation to failure due to corrosion fatigue. Other failure modes such as material degradation or mechanical shock failures are not considered.

Additionally, the corrosion fatigue process follows Jonart's six general stages as described in Figure 2-4. Once seawater penetrates the coatings and seals and contacts

sion Engineers. They frequently publish resources and Standard Practices for the corrosion industry.

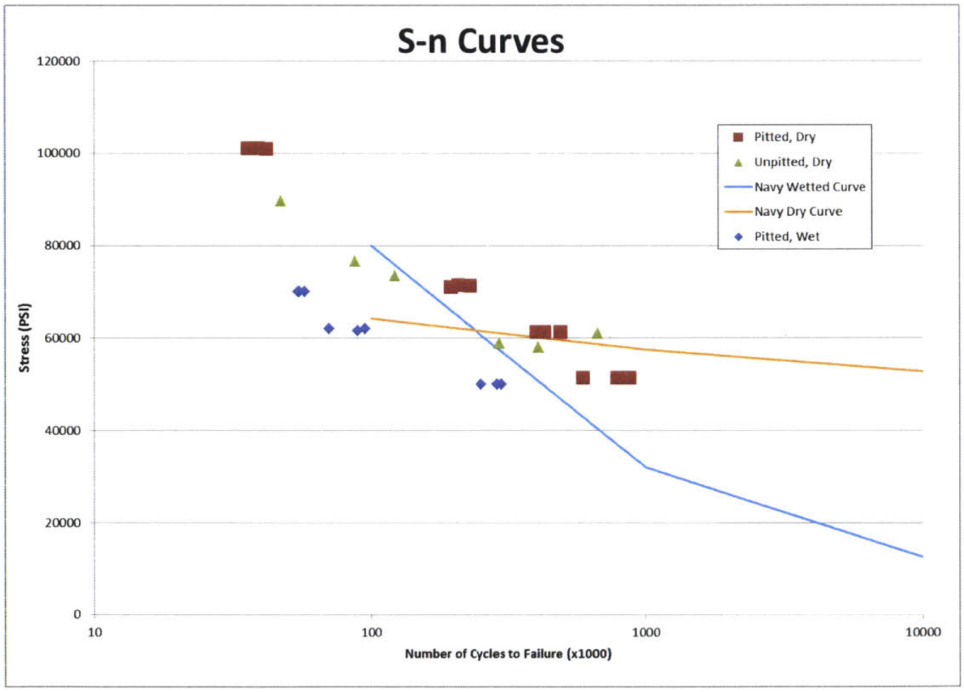

Figure 3-3: Jonart's Stress-Cycle (S-N) Curve Data [6]

the mild steel shaft, the chain begins and ultimately ends with failure. This is a conservative approach, since pits and cracks can develop and arrest, especially at loads below the fatigue limit[4]. However, studies have shown that corrosive environments essentially eliminate this limit, even though it was not initially believed to be the case [5, 9, 14]. For carbon steel in NaCl solution, Goto verified experimentally that the fatigue limit disappears [16]. Jonart, who worked with shaft steel coupons in seawater, obtained similar conclusions, illustrated in Figure 3-3 [6].

Though concepts like galvanic corrosion and CP are explicitly modeled in the corrosion fatigue process for this work, other factors like oxygen concentration, pH, and flow velocities are assumed to be incorporated into the empirical equations and constants, with only temperature distinctly present. Details and additional assumptions in modeling each of the individual stages of the corrosion fatigue chain is described in the following section.

[4]The fatigue limit, also called the endurance limit, is a term used to denote the minimum stress amplitude that can cause fatigue failure for low carbon ferritic steels. If the stress level is below the fatigue limit, micro cracks do not grow and propagate, even after an infinite number of cycles [9, 10].

3.3 The Next-Generation Submarine Propulsion Shaft Life Model

As the previous chapter mentioned, the original model treated the propulsion shaft as one object, with no distinction made between any of the submarine shaft components. Yet based on conversations with shaft inspection personnel and a review of actual submarine shaft inspection reports, most of the indications of corrosion occurred at interface points between different components of the shaft, while the span of shaft between the two bearings was largely unaffected with the possible exception of locations where holidays exist due to either imperfections in the coating or mechanical damage during installation. As such, the location of initial wetting plays a large part in corrosion fatigue rate and time to failure.

The updated model divides the shaft into four discrete parts, most notably the area just forward of the propeller (also called the propeller void), the propeller bearing, the stern tube bearing, and the coated span of shaft between the two bearings, away from any interfaces or discontinuities. Figure 2-1 depicts these typical shaft components.

However, since shaft life is solely based on corrosion fatigue, this section is broken down based on the individual phases involved in that process. To simplify the discussion, the six-stage model seen in Figure 2-4 is divided into four segments:

1. Water Ingress
2. Corrosion and Pit Nucleation
3. Pit Growth and Pit-to-Crack Transition
4. Crack Propagation to Failure

Water ingress describes the timeframe from installation needed for seawater to penetrate the protective coatings and seals around the shaft and come into contact with the mild steel. Corrosion and pit nucleation describes the subsequent timeframe, starting with the time the shaft steel becomes wetted and ending when a pit of sufficient size forms. More discussion on what constitutes "sufficient size" will follow

in ensuing sections. Pit growth and pit-to-crack transition details the period of time needed for the initial pit to grow to a threshold size, transitioning to a growing crack. The last segment, crack propagation to failure, describes the length of time needed for the crack to reach a critical size, indicating failure. The sum of all these times is the shaft life.

Each segment contains a discussion of the equations and random variable distributions used by each of the four shaft components and the literature and justification behind them.

3.3.1 Water Ingress

Since a submarine propulsion shaft is encased in a protective glass-reinforced plastic (GRP) coating, it is usually not in contact with seawater except at specific locations where this is not possible (bearing races, etc.). The expected way for the shaft to become wetted, and hence start the corrosion chain, is for seawater to permeate through the coating surface, a method that was modeled by Jonart in the original shaft life model. However, glass fiber-reinforced plastics are frequently used in marine applications due to their low water permeability [30, 31], making straightforward permeation rare. In fact, whole ships are often built out of GRP [30]. This point was reinforced during discussions with propulsion shaft experts at Portsmouth Naval Shipyard (PNSY).

Nonetheless, evidence of seawater penetration and corrosion does exist based on actual OHIO class submarine shaft inspections, typically around the problem areas delineated in Figures 2-1 and 2-5. Since the water permeability of the GRP is very low, stress and geometry factors, due to loading and the discontinuities at the interfaces, play a role in reducing the typically long water permeation times. In fact, it is not eventual water permeation that is the issue but decohesion of the interface between the GRP and locations where the GRP coating is not present. These regions are pointed out in Figures 2-1 and 2-5. As a result, each shaft component is modeled with separate and unique water ingress distributions due to the geometry and loading conditions for each area.

Additionally, within each component, the updated shaft model assumes the coating and seals can be breached via three separate mechanisms: straightforward seawater permeation, accelerated seawater permeation due to material defects or damage, and almost instantaneous permeation due to installation damage that exposes the shaft steel (which is obviously very rare but modeled for completeness).

Determining the correct random variable distributions to represent these behaviors is difficult based on the lack of open-sourced studies into the specific materials, geometry, and loading of the submarine shaft. The effects of seawater on the coating surface, for example, vary depending on the type of GRP resin used [30]. Given the absence of focused experimentation and statistical testing, a combination of Weibull and log-normal distributions were selected to model the seawater access to the shaft. Weibull distributions are common in reliability applications due to its ability to model many different life behaviors through the manipulation of its parameters [32]. Additionally, the distribution is considered "sufficiently robust to provide an adequate estimate for the statistical character of the RVs [random variables]" [17]. To represent the chances of random shaft coating defects or installation damage, a simple percentage is assumed, using inputs based on conversations with shaft inspection personnel.

Based on the large variability and complex nature of a submarine propulsion shaft, the water ingress distributions and percentages are treated as independent variables and modified as necessary to match inspection target values, similar to Jonart's original model.

The target values, as well as the water ingress distribution parameters and percentages ultimately used in the analyses, can be seen in Chapter 4.

3.3.2 Corrosion and Pit Nucleation

With the shaft steel now wetted, the uniform corrosion process can begin. In this section of the model, the time needed for a pit to form following water ingress is investigated. Again, it is prudent to point out that this pitting process is different from that seen for "classic" pitting corrosion, which as mentioned in Section 2.2 is a rapid, localized attack on small discrete areas as a result of failure of the passive

film [9]. Pitting corrosion is mainly a concern for metals that tend to develop this passivating oxide film including aluminum alloys and stainless steels [9, 10], which are not materials used in the construction of the propulsion shaft.

Corrosion pit nucleation is an electrochemical process and is largely unaffected by loading [33], which Goto observed in his carbon steel experiments [16]. However, the process is still dependent on factors and variables such as the materials and environment, with interdependencies that are not fully understood [15, 19]. As a result, most published corrosion fatigue models largely ignore the phase of pit nucleation and start with already pitted samples or artificially accelerate the pit nucleation process for the purpose of pit-to-crack transition studies [34].

One of the few models that did incorporate pit nucleation time was developed by Shi and Mahadevan, who state that the phase is best modeled with a random variable using a Weibull or log-normal distribution [19, 34]. Using a mean time of 1500 days, Shi and Mahadevan investigated three different coefficients of variation (CV) in their corrosion fatigue model based on limited data availability (1%, 5%, and 95%). For this thesis, based on the minimal amount of published literature on corrosion pit nucleation for carbon steel in seawater, a CV of 100% is used.

To account for galvanic couples and cathodic protection, based on the previously mentioned uncertainty surrounding the effectiveness of coatings and CP systems and the large variability already incorporated into the random variable, a first order approximation is utilized. Therefore, if a galvanic couple is deemed to exist, a 10% reduction in pit nucleation time is assumed. Similarly, if cathodic protection measures are in place — considering CP systems are not always impactful and the effects of cathodic disbondment and cathodic shielding on corrosion rates are difficult to estimate and vary depending on CP potential, crevice size, conductivity, pH, and even location within a crevice [26] — a 10% increase in pit nucleation time is assumed. Experiments by Varela, Tan, and Forsyth prove that within these crevices, CP current densities continually drop off with time likely due to corrosion product layer formation, in some cases all the way to zero [26], making 10% a good first order approximation in this case.

Variable	Probability
Cathodic Protection Systems Ineffective	15%
Galvanic Couple Formed at Sleeve Interfaces	80%

Table 3.1: List of Percentages Used within the Pit Nucleation Segment

The model also includes a low rate of CP inoperability, which for an assumed ICCP system means that either no protection current is being supplied or a reduced current incapable of providing sufficient protection. Similar to the chances of shaft coating defects or installation damage from the water ingress segment, this failure rate is modeled using a percentage. For the stern tube bearing and the propeller bearing, an additional percentage is used to model the chance of a galvanic couple forming following water ingress. The propeller void and shaft span do not contain the same mild steel to Alloy 625 interface, making the risk of galvanic corrosion nonexistent. A summary of the percentages used for pit nucleation are shown in Table 3.1.

3.3.3 Pit Growth and the Pit-to-Crack Transition

Now that a corrosion pit exists, the time needed to grow the pit from an initial size to a critical size can be calculated using an equation based on Faraday's Law [17, 19]. Once a critical size is reached, pit growth terminates and the pit transitions to a crack, marking the end of this segment. This segment encompasses the third and fourth phases of the six-stage corrosion fatigue process illustrated in Figure 2-4.

Using Faraday's Law, the shaft model assumes the pit grows at a constant volumetric rate ($\frac{\mathrm{d}V}{\mathrm{d}t}$) according to Equation (3.2), originally developed by Kondo [23]. This equation is very similar to Equation (3.1) introduced in Section 3.1.1, with n replacing z for valence. Substituting an Arrhenius relation in for pitting current ($I_P = I_{P0} \exp\left(-\frac{\Delta H}{RT}\right)$) and the volume of half a prolate spheroid with constant aspect ratio in for volume ($V = \frac{2}{3}\pi\phi_k^2 c^3$) yields Equation (3.3), developed by Harlow and Wei [35],

$$\frac{\mathrm{d}V}{\mathrm{d}t} = \frac{MI_P}{nF\rho} \tag{3.2}$$

$$\frac{2}{3}\pi\phi_k^2(c^3 - c_0^3) = \frac{MI_{P0}(k)}{nF\rho}\exp\left(-\frac{\Delta H}{RT}\right)t_{pg} \tag{3.3}$$

where M is the molecular weight of the material, n is the valence, $F = 96,514$ C/mole is Faraday's constant, ρ is the density, I_{P0} is the pitting current coefficient, ϕ_k is the aspect ratio, c is the pit size, c_0 is the initial pit size, ΔH is the activation enthalpy, $R = 8.314$ J/mol-K is the universal gas constant, T is the absolute temperature, and t_{pg} is the time needed for pit growth. Pitting current coefficient is a function of the number of constituent particles k, which will be discussed later in this section.

Rearranging Equation (3.3) to solve for time yields Equation (3.4), which is the time required to grow the corrosion pit from the initial size to a threshold crack initiation size [19, 35]. This equation is a simplification of Harlow and Wei's broader formula assuming a unity aspect ratio, $\phi_k = 1$, representing hemispherical pit growth [17, 33, 35]. While other pit growth models that don't assume volumetric expansion and a hemispherical shape exist, such as the model developed by Turnbull, McCartney, and Zhou on steel turbine disks, this representation is the most common and does not require complex computations [35, 36]. The equation is expressed as

$$t_{pg} = \frac{2\pi nF\rho}{3MI_{P0}(k)}(c_{ci}^3 - c_0^3)\exp\left(\frac{\Delta H}{RT}\right) \tag{3.4}$$

where c_{ci} is the crack initiation pit size and all other terms are as defined in Equation (3.3).

With the relation to calculate pit growth time now established, the next step is to determine values or random variable distributions to represent all of the terms. Some terms, such as Faraday's constant F and the universal gas constant R, have already been identified. Other terms, such as the molecular weight M, density ρ, valence

n, and activation enthalpy ΔH, can be determined based on material properties. A summary of these deterministic variables and constants and their source are shown in Table 3.3 at the end of the chapter. For the four remaining terms, large variability and uncertainty makes the modeling of each as a random variable the most appropriate solution.

The first of the terms is initial pit size, or the size of the pit created following the nucleation phase. Both Shi and Mahadevan and Harlow and Wei use the same value in their research (1.98×10^{-6} m) — a value also employed by Jonart in the original shaft model — based on experiments using aluminum alloys in corrosive environments [6, 17, 19]. The research by Turnbull et al. with steel turbine disks exposed to aerated chlorides, on the other hand, suggests that pit sizes greater than 25 μm, up to about 150 μm, mark the threshold where they become stable and start expanding. They reported that a Weibull distribution best represents this data variability while also noting that pits smaller than this threshold exist but are essentially dead pits that would no longer propagate [36]. Since these results are based on a similar steel sample, for this thesis, a Weibull distribution with a mean of 50 μm and CV = 30% is used, matching the distribution type and range described in Turnbull, McCartney, and Zhou's research.

For the critical, or crack initiation pit size, the original shaft life model used 0.5 mm based on the experiments by Fang, Eadie, Chen, and Elboujdaini on X-52 pipeline steel. However, the data is not based on a seawater environment, instead focusing on near neutral pH (NNpH) solutions sparged with a carbon dioxide gas mixture [37]. Arzaghi et al. concluded that 0.8 mm was the critical size, based on experimental data with undersea high strength steel pipelines [15]. Turnbull et al. recommend a different value, stating that at 700 μm (0.7 mm), almost all pits show corresponding cracks, with some cracks seen on pits as small as 60 μm in depth (illustrated in Figure 3-4) [36]. They again reported that a Weibull distribution best fits the data, a fact that Fang et al. also confirmed [36, 37]. By adjusting the Weibull parameters to match the data set seen in Figure 3-4, an estimated mean of 385 μm and a CV = 45% were determined.

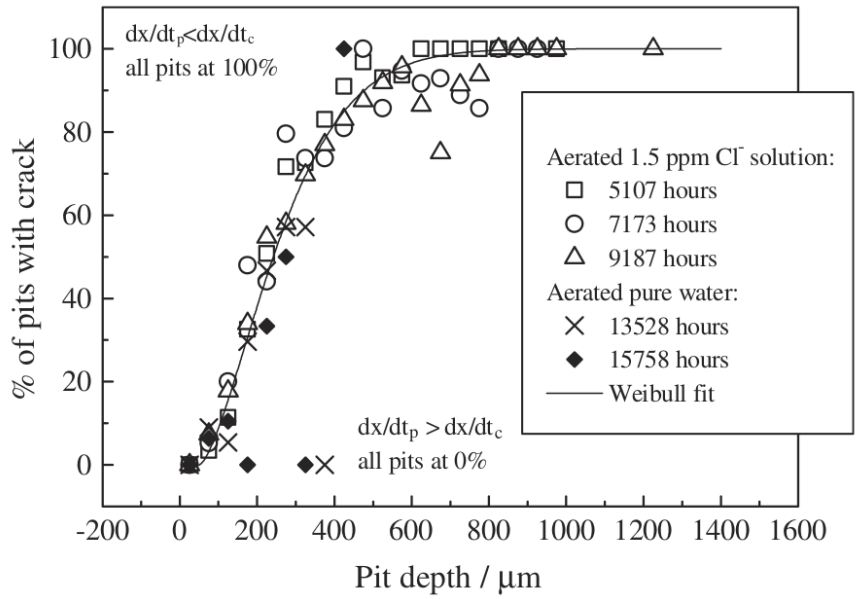

Figure 3-4: Pit-to-Crack Experimental Data in Different Environments [36]

Relationships also exist to numerically calculate the critical pit size, with Li and Akid, Huang and Xu, and Wang et al. all referencing Equation (3.5) seen below [4, 5, 38],

$$c_{ci} = \pi \left(\frac{\Delta K_{th}}{4.4 K_t \sigma_a} \right)^2 \tag{3.5}$$

where K_t is the stress concentration factor (around 2.8 for a circular hole [39]), σ_a is the stress amplitude ($2\sigma_a = \Delta\sigma$, assuming a fully-reversed stress condition $R = (\sigma_{min}/\sigma_{max}) = -1$), and ΔK_{th} is the threshold stress intensity factor, or driving force, seen in Figure 3-5.

Using a ΔK_{th} of 8 MPa$\sqrt{\text{m}}$ (derived from Figure 3-5) and a $K_t\sigma_a$ of 96 MPa[5], a critical pit size of approximately 360 μm is calculated, which is a similar value to those obtained by previous researchers and matches very closely the mean value found by Turnbull et al. Some of the difference in value can be attributed to stress

[5]This value comes from combining the maximum bending and shear stress values in Table 3.3 and dividing by two to obtain stress amplitudes (assuming $R = -1$). The stress values were obtained from the doctoral dissertation of Douglas Jonart (MIT), Reference [6], and are inclusive of stress concentration factors.

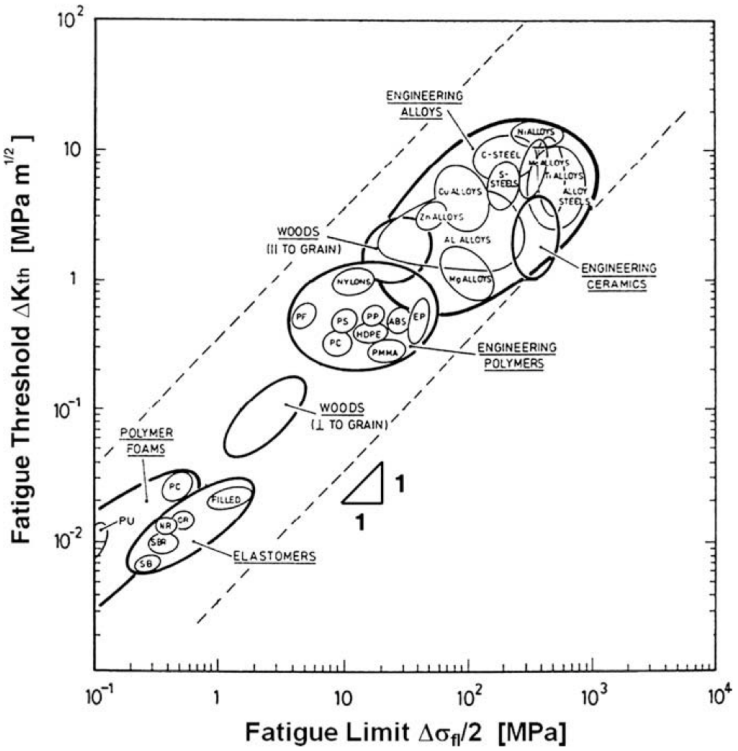

Figure 3-5: Fatigue Threshold vs. Fatigue Limit for Various Materials [40]

range. Goto empirically determined that the critical pit size can vary from 100 μm at 300 MPa to only 25 μm at 500 MPa, with variance increasing for lower stresses [16]. For the purposes of the updated shaft model, critical pit size once more follows the Weibull distribution determined by Turnbull et al.

For the pitting current coefficient I_{P0}, its estimation has significant uncertainty due to pitting complexities, accurate measurement difficulties, and lack of actual environmental history [39]. Even Harlow and Wei utilized three different statistical distributions, with three different mean values, in each of the three articles referenced in this thesis [17, 35, 39]. The most prevalent model is based on the number of constituent particles k, which represent heterogeneities on the material surface from which corrosion pits usually initiate [41]. Steel contains a large number of these particles [41], which can be modeled using the Pareto distribution described by Harlow and Wei in their 1998 study [35]. The study also contains the equations and Weibull parameters needed to calculate the pitting current coefficient from the number of constituent particles, as seen in Equation (3.6). A summary of the random variable

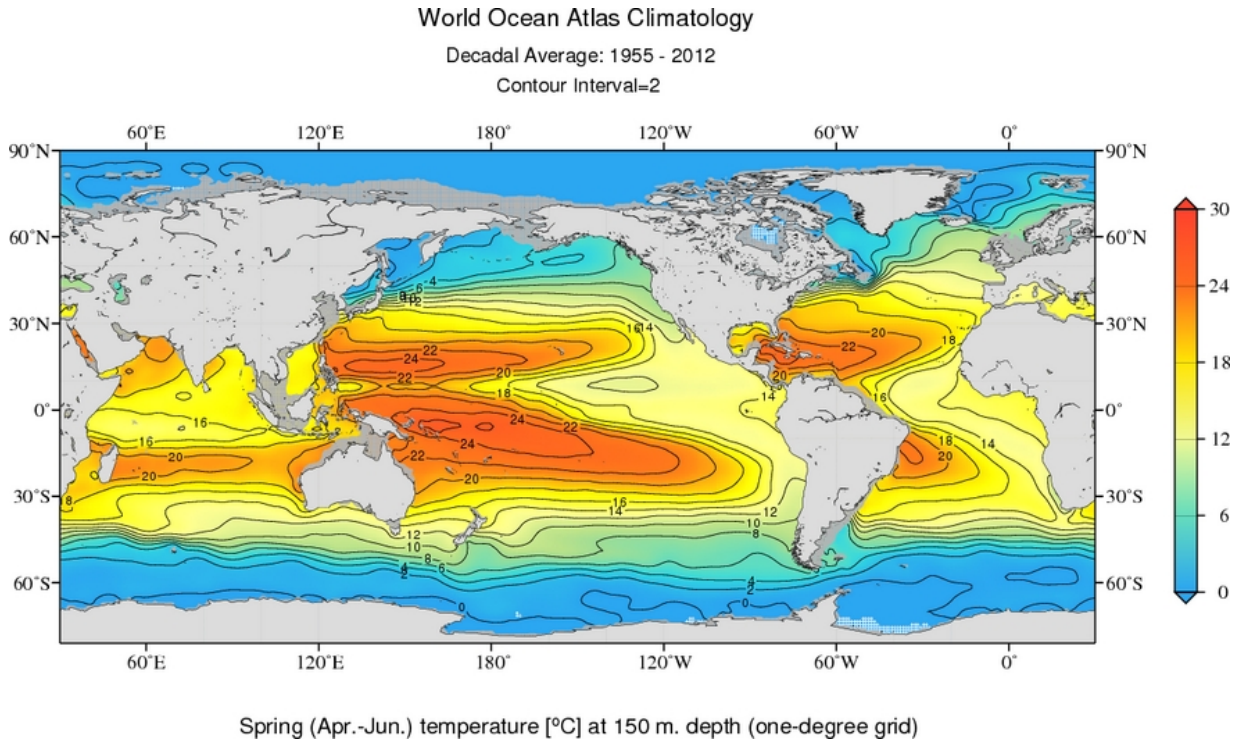

Figure 3-6: Decadal Average Seawater Temperature at a Depth of 150 meters [42]

distributions and CVs used for both k and I_{P0} can be seen in Table 3.2.

$$I_{P0} = (k+1) \cdot 6.5 \times 10^{-5} \text{ C/s} \tag{3.6}$$

The last term to be resolved is absolute temperature. Using the World Ocean Atlas 2013 from the National Oceanic and Atmospheric Administration (NOAA), average seawater temperatures for a range of ocean depths can be acquired. As a default, temperature at a water depth of 150 meters is used for this thesis, seen in Figure 3-6. At this depth, the average temperature appears to range from about 5 to 25 degrees Celsius (278 to 298 K) for most of the oceans. As such, the absolute temperature input into the pit growth equation follows a normal distribution with a mean of 288 K. However, the probabilistic submarine shaft model allows an operator to quickly and easily adjust seawater depth to either 100, 150, or 200 meters, with the appropriate seawater temperature distribution subsequently inputted into the equation.

Once critical pit size is reached, it is assumed that the two corrosion fatigue

requirements needed for a pit to transition into a crack are fulfilled [5, 15, 19, 38]. The requirements are stated below, quoted from Li and Akid.

1. The stress intensity factor of the equivalent surface crack has reached the threshold stress intensity factor for fatigue crack growth, assuming that a corrosion pit may be modeled by an equivalent semi-elliptical surface crack. $\Delta K_{pit} = \Delta K_{th}$

2. Corrosion fatigue crack growth rate exceeds the pit growth rate. $(\frac{\mathrm{d}a}{\mathrm{d}t})_{crack} \geq (\frac{\mathrm{d}a}{\mathrm{d}t})_{pit}$

These first three segments of the corrosion fatigue chain encompass a lot of variability, yet they also typically comprise the majority of the fatigue life [38]. Recommendations and potential methods to reduce some of this uncertainty are given in Section 5.2.

3.3.4 Crack Propagation and Failure

Numerous researchers have investigated the dynamics of fatigue crack propagation, with some, including Shi and Mahadevan, dividing the process into two regimes — a faster short crack growth and the more defined long crack growth [19]. However, while there is some consensus that a separate regime exists, Arzaghi et al. pointed out that there is no explicit short crack growth formula [15]. Both studies do agree that a probabilistic equation based on Paris' Law can be applied, so long as the uncertainty in the terms is accounted for [15, 19]. The most common Paris model for damage growth is expressed as

$$\frac{\mathrm{d}a}{\mathrm{d}N} = C(\Delta K)^m \tag{3.7}$$

where $\frac{\mathrm{d}a}{\mathrm{d}N}$ is the crack growth rate, ΔK is the stress intensity factor, and C and m are Paris constants representing the intercept and slope terms respectively.

The widely used Paris Law approximation works well for most fatigue crack simulations, though its application is best suited for Stage II of a typical fatigue crack

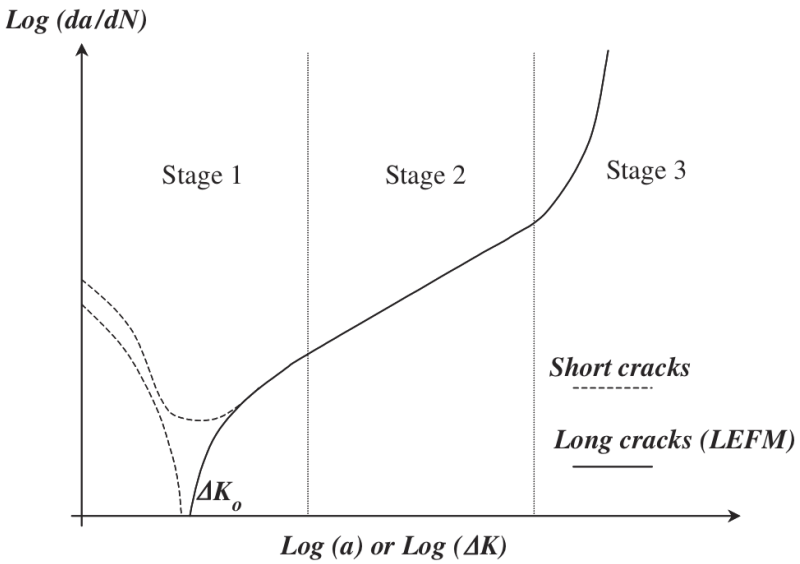

Figure 3-7: Typical Fatigue Crack Growth Behavior [43]

curve, shown in Figure 3-7 [43]. As the crack length and stress intensity factor increase, so too does the crack growth rate.

To calculate the stress intensity factor ΔK, Tada, Paris, and Irwin's crack handbook was referenced in order to obtain equations for a shaft-like external crack on a thick-walled cylinder, instead of the usual infinite plate simplification used in most studies [44, p. 408]. Calculations for stress intensity factor as well as stress, are shown in Equations (3.8) and (3.9),

$$\Delta K = \Delta\sigma\sqrt{\pi a} \cdot \alpha \left(\frac{r_i}{r_o}, \frac{a}{t} \right) \tag{3.8}$$

$$\sigma_a = \frac{4 M_t r_o}{\pi \left(r_o^4 - r_i^4 \right)} \tag{3.9}$$

where r_o is the shaft outer radius, r_i is the shaft inner radius, M_t is the moment, σ_a is the applied stress, a is the depth of the crack, t is the thickness of the shell, and α is a correction factor based on the ratios between radii and depth to thickness. Again assuming a fully reversed stress condition ($R = -1$), $\Delta\sigma = 2\sigma_a$. As Equation (3.9) shows, the applied stress depends on the total moment, indicating that shaft location

will play a role in the rate of crack growth.

After substituting Equation (3.8) back into Equation (3.7), a relation for the number of cycles needed for a crack to propagate from an initial size to a critical size results, sometimes called the remaining useful life (RUL) [45, 46, 47],

$$N_f = \frac{a_c^{1-m/2} - a_i^{1-m/2}}{C\left(1 - \frac{m}{2}\right)\left(\alpha \cdot \Delta\sigma\sqrt{\pi}\right)^m} \tag{3.10}$$

where N_f is the number of cycles until failure, a_c is the critical crack size denoting failure, a_i is the initial crack size, $\Delta\sigma$ is the stress range, α is the correction factor, and C and m are the Paris parameters.

One modification was made to the equation in order to incorporate the correction factor needed to model a cylindrical geometry, shown by the addition of the α term. For this thesis, a correction factor of 0.67 is used to represent a semi-circular crack [48].

Additionally, initial crack size is assumed to be the same as the critical pit size, and failure crack size is assumed to be the circumference of the submarine shaft, approximated at 1.7 m based on a 21 inch diameter [6].

Paris parameter m was obtained using Figure 3-8, which resulted in a range of about 2.2 to 4. This range agrees with the typical values exhibited by most metals (usually 2 to 4) [49] and is simulated using a uniform distribution in the updated shaft model.

For the Paris parameter C, a mean of 1.4×10^{-11} is used based on studies by Mlikota, Staib, Schmauder, and Božić using carbon steel specimens [49]. Li and Akid derived a similar value for their carbon steel shaft experiments in seawater, for both the short and long crack regimes [5]. Based on the ranges typically found in literature, the parameter is modeled using a normal distribution with a CV = 25%.

The last term to analyze for in order to calculate RUL is the stress range, which, as already mentioned, depends on component location. According to Jonart, the maximum bending stress specified by the Navy is 6000 psi, or about 41 MPa [6]. He also calculated the max shear stress due to torsion, which is 2.19×10^4 psi, or about

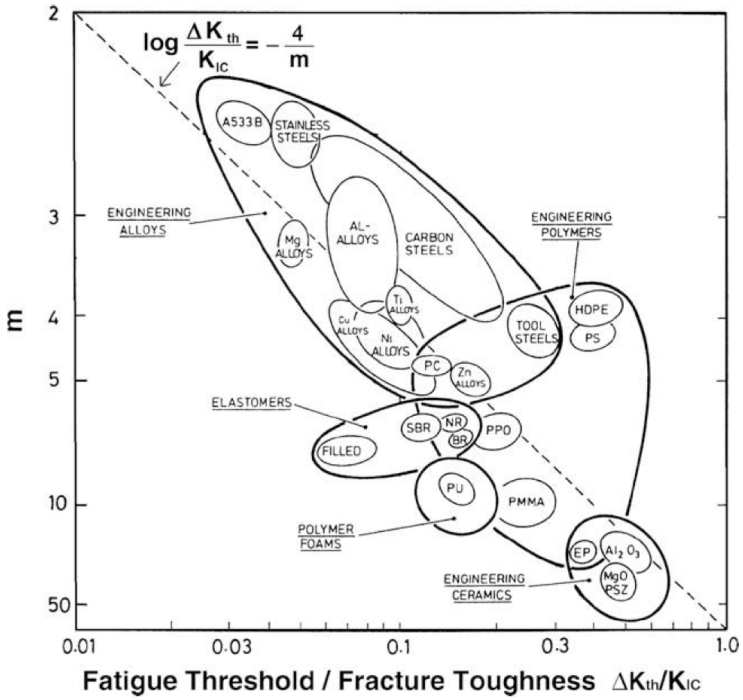

Figure 3-8: Paris Parameter m vs. Fatigue Threshold / Fracture Toughness [40]

151 MPa [6]. Using a simple summation of bending and shear stress, the maximum stress range equals 192 MPa. However, not all shaft components will experience this maximum value.

The largest stress ranges are likely experienced by the aft end of the shaft, where the weight of the propeller has the largest impact. As a result, for the propeller void and the propeller bearing, the maximum 192 MPa is conservatively used as the stress range mean, using a log-normal distribution and applying a CV = 25%. For the stern tube bearing, it is assumed that the bending stress experienced is half of the maximum, or about 20 MPa. Combined with the maximum shear stress, a stress range of 171 MPa is obtained, again applying a 25% coefficient of variation. For the last shaft component, the span of shaft between the bearings, the model assumes that the stress range is a result of torsion only, using a mean of 151 MPa.

With the number of cycles to failure calculated, the process of converting that value to a unit of time is fairly straightforward. Two additional terms are needed: an average number of shaft revolutions per minute (RPM) and a Naval term called operational tempo, or OPTEMPO, which describes the fraction of time that a ship

or submarine spends out at sea. Simply dividing RUL by RPM assumes that the shaft is continuously rotating, which is not the case. For the purposes of this thesis, an average RPM of 50 fatigue cycles/minute is assumed with an OPTEMPO of 0.5. However, these values, much like the average seawater depth, can be easily modified in the shaft life model, as Section 3.4 will show.

3.3.5 Summary of Model Variables

All of the random variable distributions, with the exception of the water ingress distributions, are summarized in Table 3.2 with their mean and coefficients of variation (CV). A review of all the constants and deterministic values used for the submarine shaft life model are shown in Table 3.3. The water ingress values are discussed in Chapter 4.

Random Variable	**Distribution**	**Mean**	**CV %**
Pit Nucleation Time	Weibull	1500 days [19]	100
Initial Pit Size c_0	Weibull	50 μm [36]	30
Critical Pit Size c_{ci}	Weibull	385 μm [36]	45
Number of Constituent Particles k	Pareto (truncated)	4.4 [35]	102
Pitting Current Coefficient I_{P0}	Weibull	$(k+1)6.5 \times 10^{-5}$ C/s [35]	108
Absolute Temperature T	Normal	288 K [42]	1.7
Paris Parameter C	Normal (truncated)	1.43×10^{-11} [49]	25
Paris Parameter m	Uniform $(2.2 - 4)$	3.1 [40]	16.8
Stress Range $\Delta\sigma$	Log-Normal	Location Dependent	25

Table 3.2: List of Random Variables Used

Variable	Value
Valence n	2 [6]
Faraday's Constant F	96485 C/mol [38]
Molecular Weight M	55.845 g/mol [6]
Density of Steel ρ	8000 kg/m^3 [6]
Universal Gas Constant R	8.314 J/mol-K [19]
Activation Enthalpy ΔH	26.74 kJ/mole [50]
Shaft Inner Radius r_i	14 cm [6]
Shaft Outer Radius r_o	27 cm [6]
Shaft Thickness $t = r_o - r_i$	13 cm
Initial Crack Size a_i	(same as crit. pit size)
Critical Crack Size a_c	$2\pi r_o = 1.696$ m
Stress Concentration Factor K_t	2.8 [39]
Max Shear Stress (Torsion)	2.19×10^4 psi [6]
Max Bending Stress	6000 psi [6]
Geometry Correction Factor α	0.67 [48]
Threshold Stress Intensity Factor ΔK_{th}	8 MPa$\sqrt{\text{m}}$ [40]
Average RPM	50 revolutions/minute
Operational Tempo (OPTEMPO)	0.5

Table 3.3: List of Constants and Deterministic Variables Used

3.4 The GoldSim Model

With the mathematical relationships for the corrosion fatigue behavior of propulsion shafts determined, the next step is to build and exercise the model using Monte Carlo simulation. For this thesis, the GoldSim software platform was used. A screenshot of the top layer of the model is shown in Figure 3-9 with the secondary component-level layer, obtained by expanding the Propulsion Shaft icon in the top view, shown in Figure 3-10. Figure 3-11 shows the corrosion fatigue framework within a single

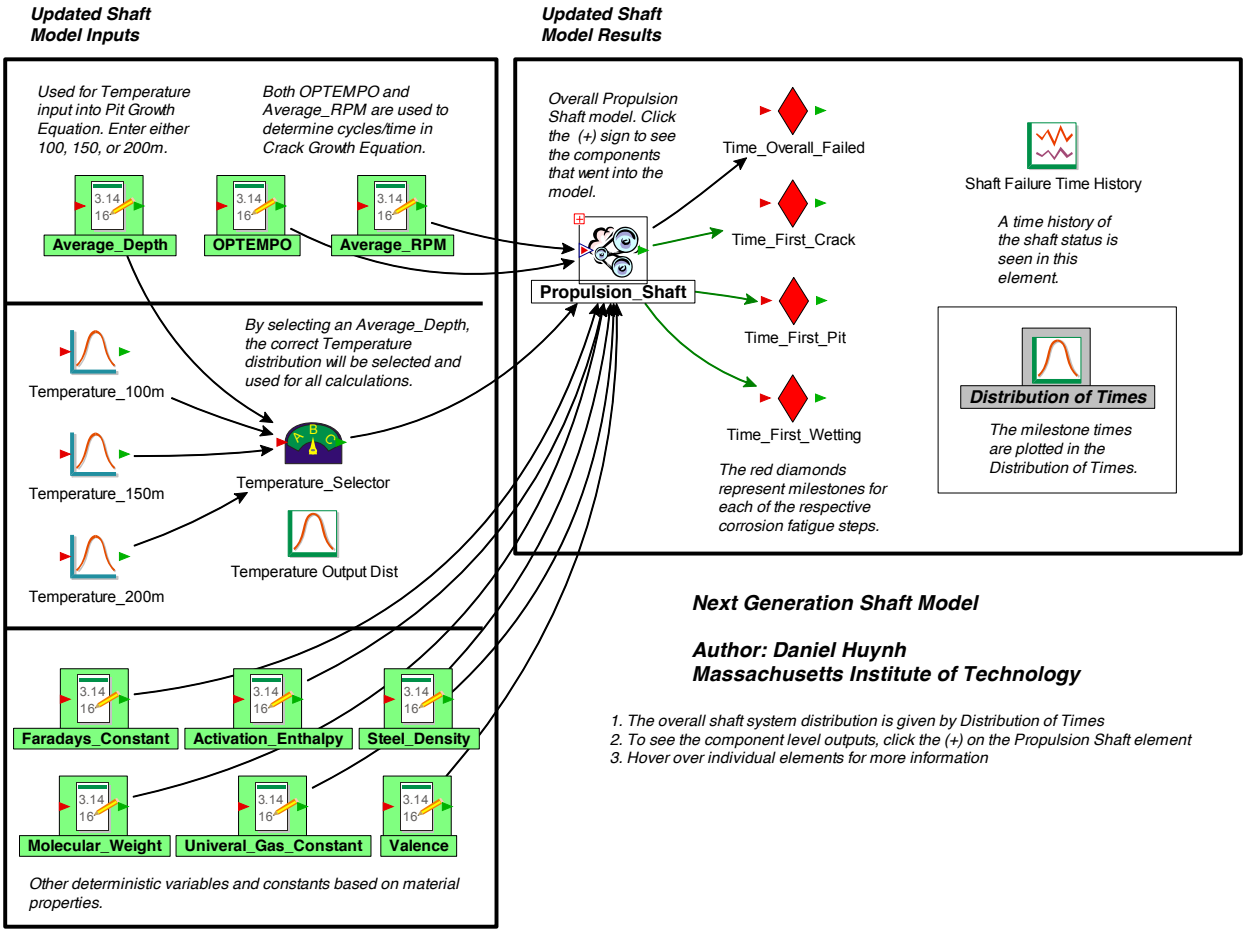

Figure 3-9: GoldSim Submarine Shaft Life Model - Top View

shaft component, in this case the propeller bearing. Similar frameworks can be found by expanding any of the other three modeled shaft components. A more detailed description of the GoldSim program is provided in Appendix A.

The model currently has nine easily-modifiable inputs which are highlighted in green in Figure 3-9. The three terms at the top are operation-based inputs while the six terms at the bottom represent constants and properties of the shaft material in use. By adjusting any of the values, all equations using the terms are simultaneously altered, with the output revised accordingly. Only three depth inputs (100, 150, and 200 meters) are presently offered, though more can be built using data from NOAA's World Ocean Atlas. Figure 3-10 also shows how the model can easily be modified to incorporate new shaft components, with strut bearings, couplings, and seals representing possible options.

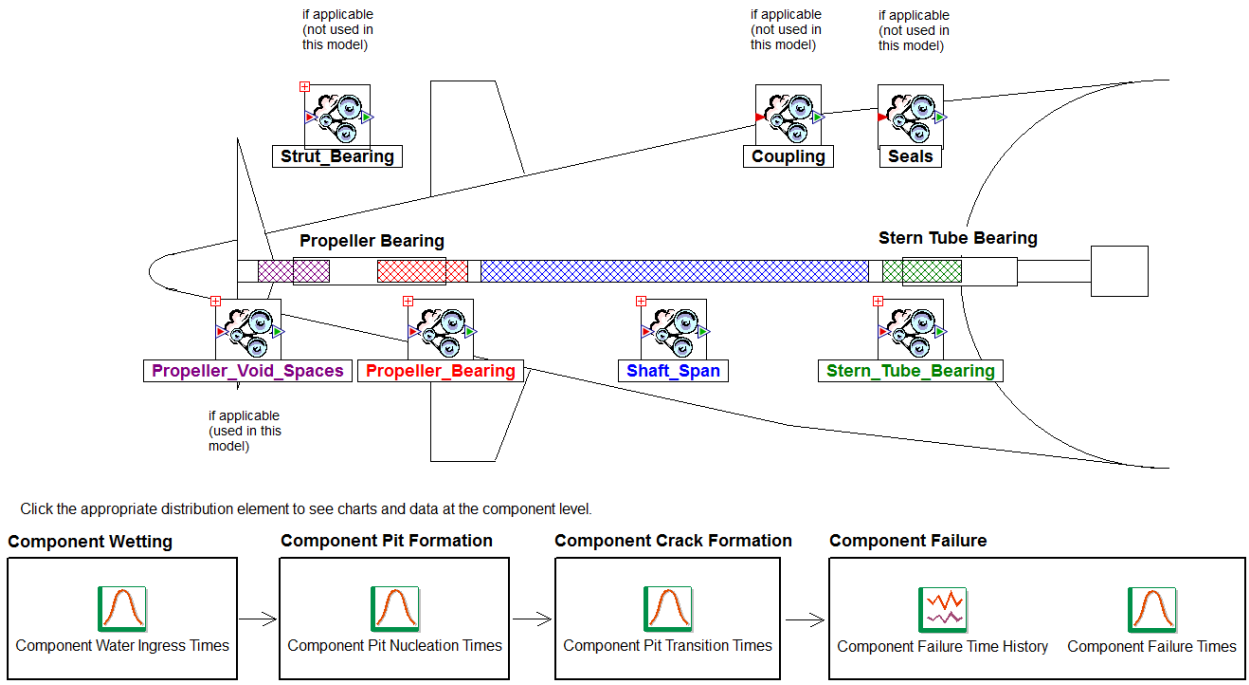

Figure 3-10: GoldSim Submarine Shaft Life Model - Component View

3.5 Chapter Summary

As this chapter demonstrates, many variables and statistical distributions are necessary in the development of the probabilistic submarine shaft life model. While each shaft component essentially undergoes the same corrosion fatigue process from water ingress to failure, details such as varying stress ranges and the presence of galvanic couples can significantly impact predicted shaft life. By dividing the shaft into smaller elements, these factors can easily be incorporated. Additionally, a Monte Carlo simulation program like GoldSim greatly simplifies the modeling, even with the increased detail and complexity of having each shaft component experiencing a separate corrosion fatigue process, an advantage the original model did not have. While the number of shaft components modeled in this thesis is by no means exhaustive, additional components can easily be created and added to the model, a fact that is covered in more detail in Chapter 5.

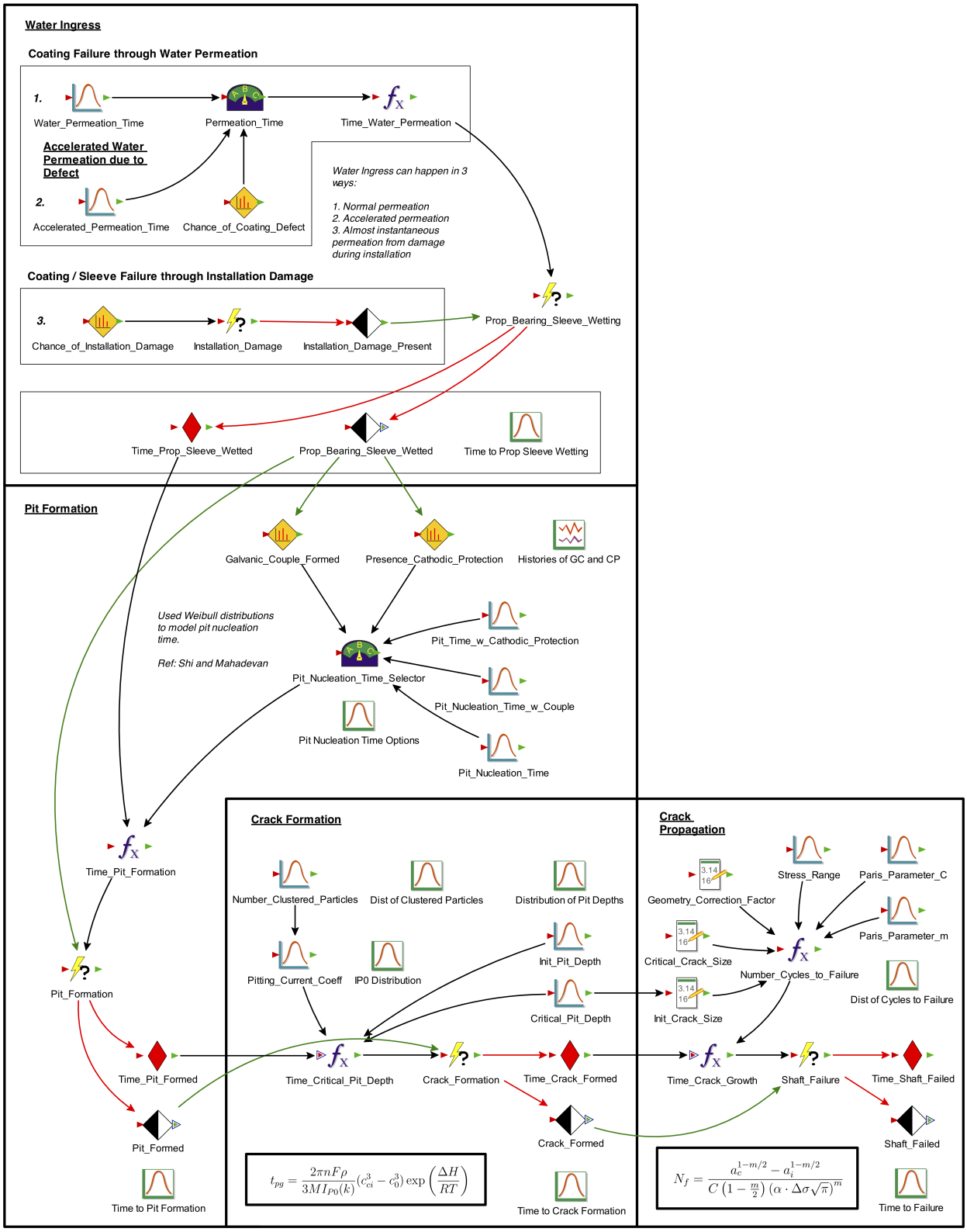

Figure 3-11: GoldSim Submarine Shaft Life Model - Propeller Bearing View

THIS PAGE INTENTIONALLY LEFT BLANK

Chapter 4

Results and Observations

With the probabilistic model now constructed, this chapter describes the target values and Monte Carlo parameters needed to perform the simulations and obtain a shaft life prediction. Taking advantage of the computing power of the GoldSim software, the complex probability computations that Harlow and Wei had to perform, such as employing the change-of-variable theorem for multidimensional random variables, were avoided [17, 35]. After a review of the results, an analysis on the sensitivity of the output to input variability is provided, followed by a discussion of model limitations and uncertainty.

4.1 Target Value Selection

In order to calibrate the corrosion fatigue life predictions, first simulation target values have to be selected. Ideally, these target values represent the "expected" outcomes at a specified time based on a review of actual shaft inspection information, allowing the model to be anchored to a set of real-world data points. However, for the purposes of this thesis, the same hypothetical target values employed in Jonart's original shaft model are used for this updated study. The values are summarized in Table 4.1.

These target values represent the percentage of all shafts that could expect to see the listed conditions at the 6-year operational interval. It is important to note that these numbers are only approximations. A more detailed and precise set of target

Condition	Probability (% of Total)
Wetted	70%
Pitted	40%
Cracked	4%
Failed	0%

Table 4.1: Model Simulation Condition 6-year Target Values

values would immediately improve the accuracy of the results. However, obtaining accurate values from inspection data can be difficult, considering some of the defects over long fatigue lives form below the surface and are not easily visible [14].

It is also important to understand that these target values apply to the shafting system as a whole and not to each specific shaft component in the model, especially since some areas and components are of particularly more concern than others. A more thorough explanation is given with the simulation results in the subsequent sections.

4.2 Water Ingress Calibration

As Section 3.3.1 discussed, the dynamics of water ingress on a submarine propulsion shaft are not easily computed. It requires an understanding of the precise geometry and conditions at each of the joints and interfaces, information not readily available without specific knowledge or experimentation. However, approximations can be made using random variable distributions and percentages in order to resemble actual results. In this study, the target values seen in Table 4.1 represent the "actual" results.

Since 70% of all shafts inspected at the 6-year interval exhibit wetting, the distribution parameters and defect percentages were adjusted using basic statistical methods in order for the overall shaft model to achieve the same 70% water ingress probability after six years. The distributions, along with their respective means and coefficients of variation (CV), are shown in Table 4.2. The probabilities of defects and installation damage are summarized in Table 4.3.

Random Variable	Distribution	Mean	CV %
Propeller Void Spaces			
Seal Failure Time	Weibull	12 yrs	80
Accelerated Seal Failure Time	Weibull	8 yrs	80
Propeller Bearing Sleeve Interface			
Water Permeation Time	Weibull	12 yrs	80
Accelerated Permeation Time	Weibull	8 yrs	80
Shaft Span			
Water Permeation Time	Log-Normal	25 yrs	50
Accelerated Permeation Time	Log-Normal	20 yrs	50
Stern Tube Bearing Sleeve Interface			
Water Permeation Time	Weibull	12 yrs	80
Accelerated Permeation Time	Weibull	8 yrs	80

Table 4.2: List of Water Ingress Random Variables Used

Variable	Probability
Coating or Seal Defect Present	5%
Installation Damage Exposing Shaft Steel	0.5%

Table 4.3: List of Percentages Used within the Water Ingress Segment

4.3 Monte Carlo Simulation

Monte Carlo simulations are frequently used in reliability engineering because they not only provide numerous statistical analyses like means and confidence intervals for the system in question, but they can also reveal unique failure mechanisms not previously identified through simulation across the entire range of input options [51]. These simulations are made easier through the use of a software program, which for this thesis is the platform GoldSim. As mentioned earlier, GoldSim is described in more detail in Appendix A.

Inputs needed to perform the simulation include time duration, time step, and the number of realizations, which represents the number of independent runs through the fatigue life model. In this study, 1000 shaft realizations were conducted, simulating 1000 different submarine shafts undergoing the probabilistic, corrosion fatigue process, each independently sampling from the range of possible options for each variable. Other simulation parameters used include a time duration of 2000 years and a time step of 6 months. The time duration was chosen specifically to maximize the data, since some of the simulated shaft failure times approached this value based on the large amount of uncertainty. A shorter time duration would cut off these realizations, essentially eliminating the data point.

At the conclusion of the simulation, tables, graphs, and analyses for almost every model variable were obtained. However, for this thesis, the main outputs desired are the probability density functions (PDFs) and cumulative distribution functions (CDFs) for each of the corrosion fatigue milestones — wetting, pitting, cracking, and failure. These plots were produced for the submarine shaft system as a whole as well as for each of the individual shaft components, making data comparison and identification of problem components possible.

4.4 Prediction of Propulsion Shaft Life

This section highlights some of the CDFs obtained after running the Monte Carlo simulation for submarine propulsion shaft life, with the 6-year and 12-year intervals specifically identified in the results. First a component-by-component view is analyzed, noting differences in corrosion fatigue life in each segment, followed by the overall shaft system analysis.

4.4.1 Component Level Analysis

The first diagram (Figure 4-1) depicts the probability of water ingress for each of the four modeled shaft components. Noticeably, only the span of shaft between the bearings differs from the others, based on the different seawater permeation times

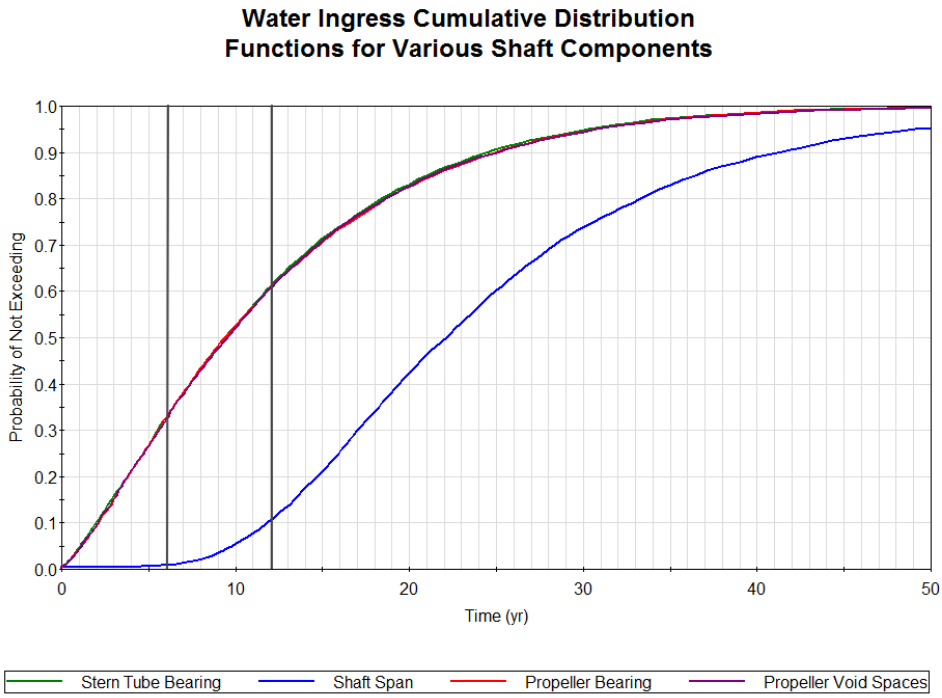

Figure 4-1: GoldSim Water Ingress Distribution

used in the model. This distinction matches expectation since the conversations with inspection personnel and inspection report reviews indicated that evidence of corrosion on the shaft span is rare at the 6-year interval. It can also be seen that the probability of water ingress for each component is not 70% per the target values in Table 4.1. This is again because the figure depicts the probability that a single shaft component becomes wetted, while the target values apply to the shafting system as a whole.

During the pit nucleation phase, the results of which are shown in Figure 4-2, a significant variation begins to appear on the CDFs since components like the propeller and stern tube bearings can develop galvanic couples, accelerating corrosion fatigue. With the exception of the shaft span, the probability of each component developing a pit at the 6-year interval lies at around 15%, with the probability jumping to almost 45% at the 12-year interval.

A similar trend is observed during the pit growth and transition segment as shown in Figure 4-3. The variations become compounded by the large uncertainty inherent to

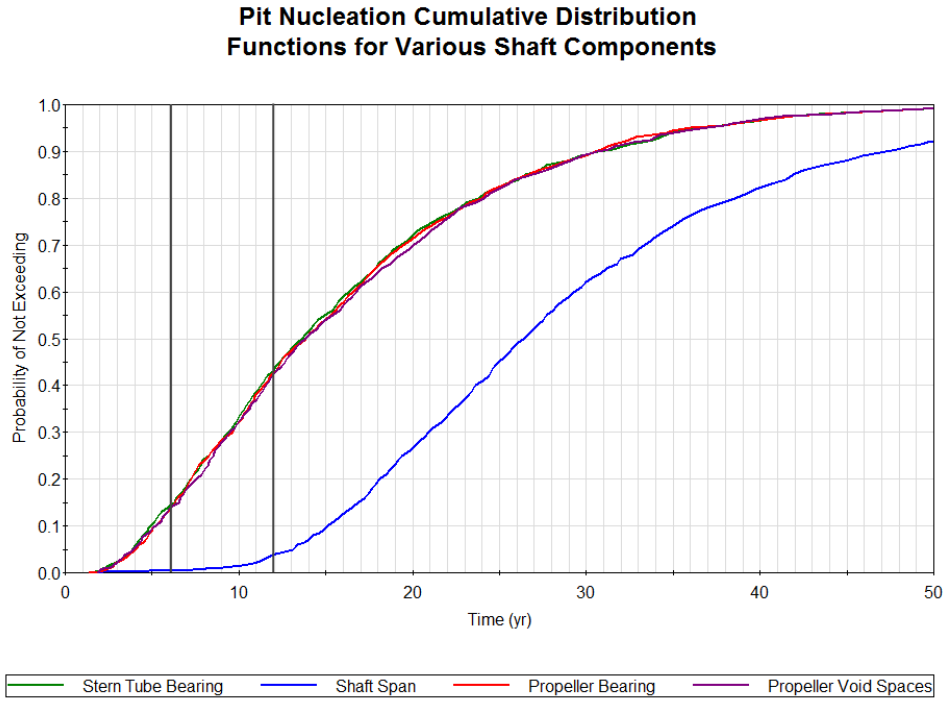

Figure 4-2: GoldSim Pit Nucleation Distribution

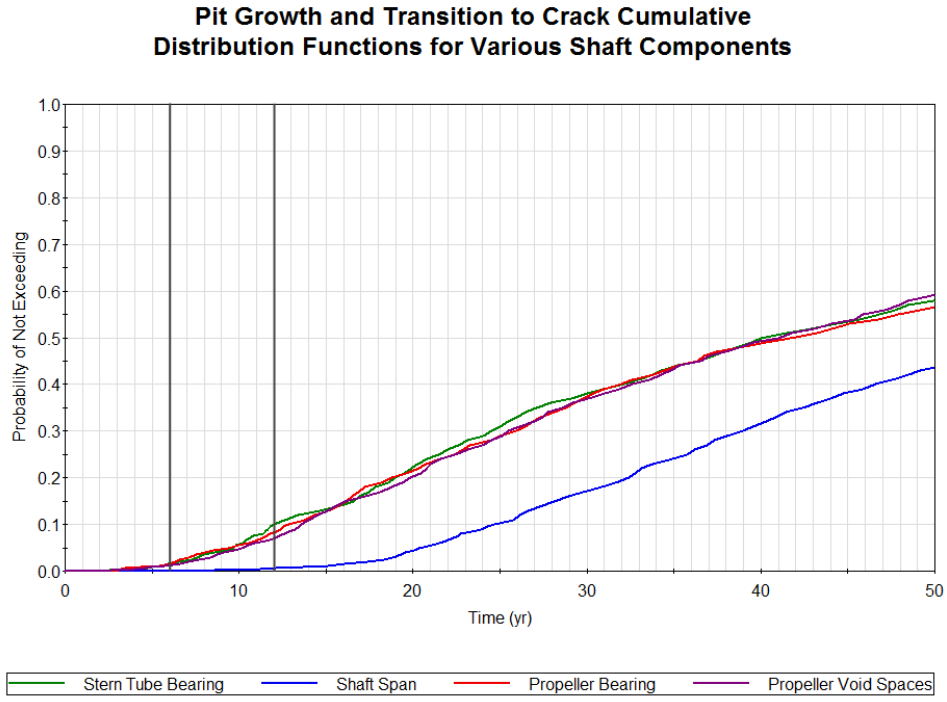

Figure 4-3: GoldSim Pit Growth and Transition to Crack Distribution

most of the terms in the pit growth relationship. The phase ends with the development of a fatigue crack, with notably lower probabilities observed.

In the last phase, the results of which are shown in Figure 4-4, not much difference is observed with the previous phase, with the probability of failure following crack growth essentially equaling the probability of crack formation following pit growth. This is due to the relatively short amount of time it takes for the crack to propagate around the circumference of the shaft, as modeled using Paris Law. As a result, the probability that a single component fails after 6 years is around 2%, shaft span aside. The probability rises to just under 10% after 12 years. It should be noted that the actual load-time history as well as an accurate data set for this history control this phase. An analysis of a real submarine shaft system would require a very accurate load-time history — which predictably would be classified. Moreover, the data set should include the combined effects of both bending and torsion (the actual in-service conditions), which will likely have an effect on not only crack growth, but also on the time to water ingress at the key interfaces between the GRP and the bearing sleeve.

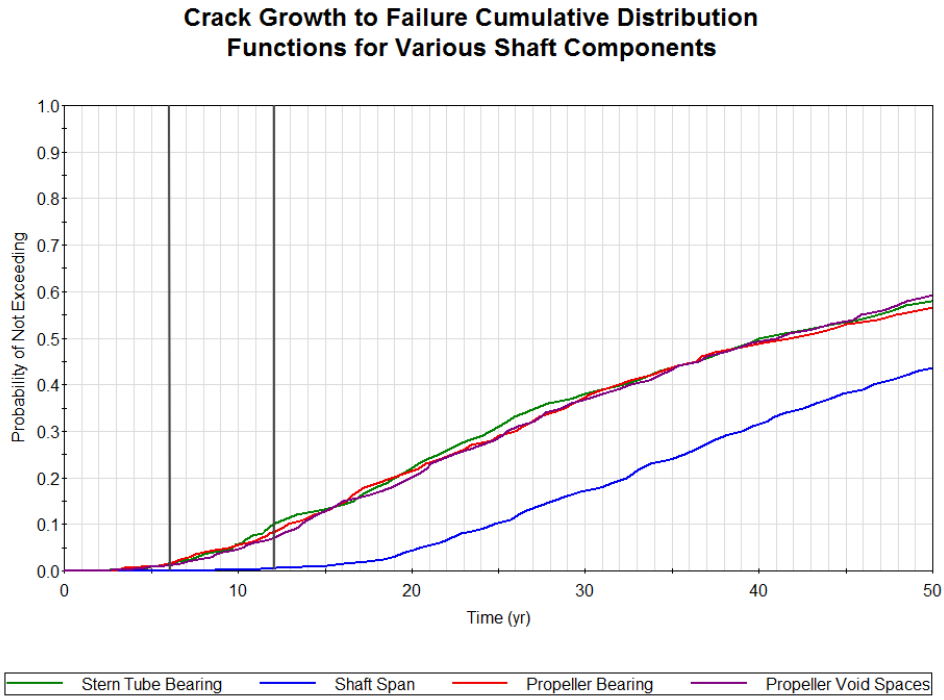

Figure 4-4: GoldSim Crack Growth to Failure Distribution

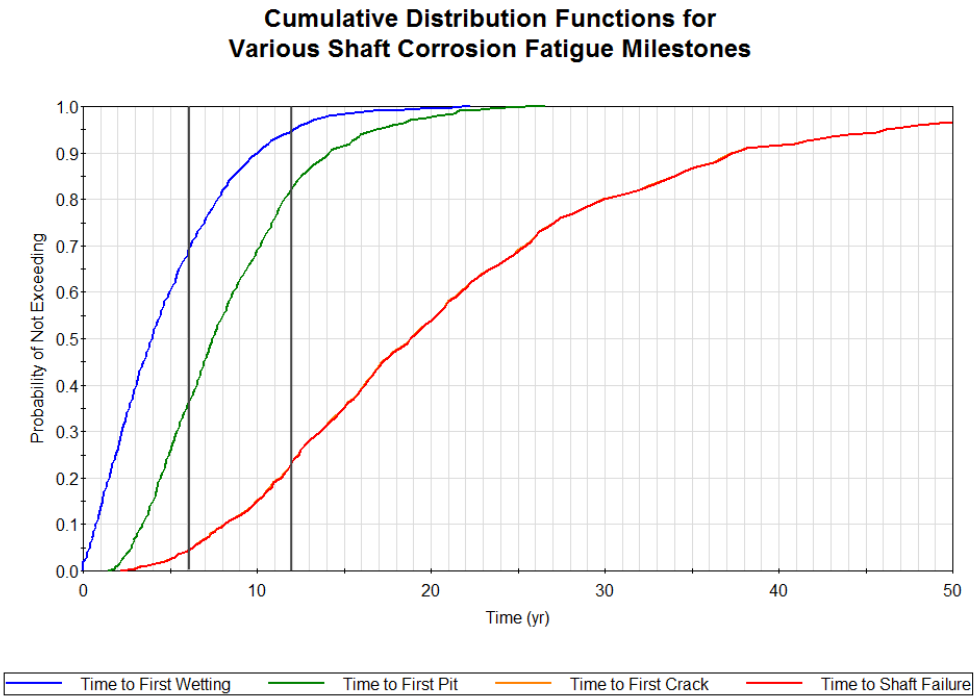

Figure 4-5: GoldSim Propulsion Shaft Failure Distribution

4.4.2 System Level Analysis

While a component level analysis is beneficial for comparisons and the localization of problem areas, the main statistic of concern is whether the submarine shafting system as a whole will fail.

The results of the Monte Carlo simulation, as viewed with respect to the entire system, are shown in Figure 4-5. The CDF was developed using a bottom-up approach. Whenever a single component within the shaft system experiences water ingress, pitting, cracking, or failure, then the whole propulsion system is considered wetted, pitted, cracked, or failed. As a result, even though the probability of any single shaft component becoming wetted at 6 years is less than 35% (shown in Figure 4-1), the probability of the shafting system becoming wetted at 6 years is 70%, matching the target value. Similarly, the probability of the shaft as a whole becoming pitted or cracked after 6 years is about 37% and 4%, respectively, with the probability of failure also at about 4%. A summary of the 6-year inspection interval probabilities is shown in Table 4.4, together with the model target values.

Condition	**Probability (Simulation)**	**Probability (Target)**
Wetted	70%	70%
Pitted	37%	40%
Cracked	4%	4%
Failed	4%	0%

Table 4.4: Actual Simulation Probabilities vs. Target Values at a 6-year Inspection Interval

One notable point seen in the table is that the simulation results do not resolve any separation between time of crack initiation and time of failure, since application of a Paris model combined with a high average shaft RPM (fatigue cycles/minute) results in very fast crack propagation. As a result, most of the shaft life is taken up by the phases prior to crack propagation (i.e. the first three segments), which corresponds well to the findings of Pérez-Mora et al., who concluded that over 95% of fatigue life is consumed in crack initiation when compared with crack propagation in high cycle testing [14]. It should be noted, however, that should an actual load-time history be applied, the results would likely not be as extreme.

Based on the observed data at 6 years, at a 12-year inspection interval, the probability of propulsion shaft wetting elevates to 95%, with probabilities of pit and crack initiation similarly raising to 82% and 23%, respectively. Again, since crack propagation occurs quickly, the probability of shaft failure at the 12-year inspection interval is just under 23%.

Compared with the results from Jonart's original shaft life model, the risk of failure after 12 years has decreased from 45% to 23%, assuming no changes have been made to the propulsion shaft design. However, the probabilities of water ingress and pit formation have substantially increased, summarized in Table 4.5.

While the decrease in failure probability may seem like a substantial improvement, having almost a one in four chance of propulsion shaft failure after 12 years is obviously still not acceptable.

Condition	Original Model	Next Generation Model
Wetted	87%	95%
Pitted	69%	82%
Cracked	59%	23%
Failed	45%	23%

Table 4.5: Comparison of Probabilities from Original to Next Generation Shaft Model at a 12-year Inspection Interval

4.5 Sensitivity Analysis

Another benefit of the GoldSim platform is its ability to easily perform sensitivity analyses. Since shaft system failure time is the variable of interest, the model can sequentially vary all the other random variables through the range of possible values and determine its individual effect on the failure time. The results of this analysis are shown in Figures 4-6 and 4-7.

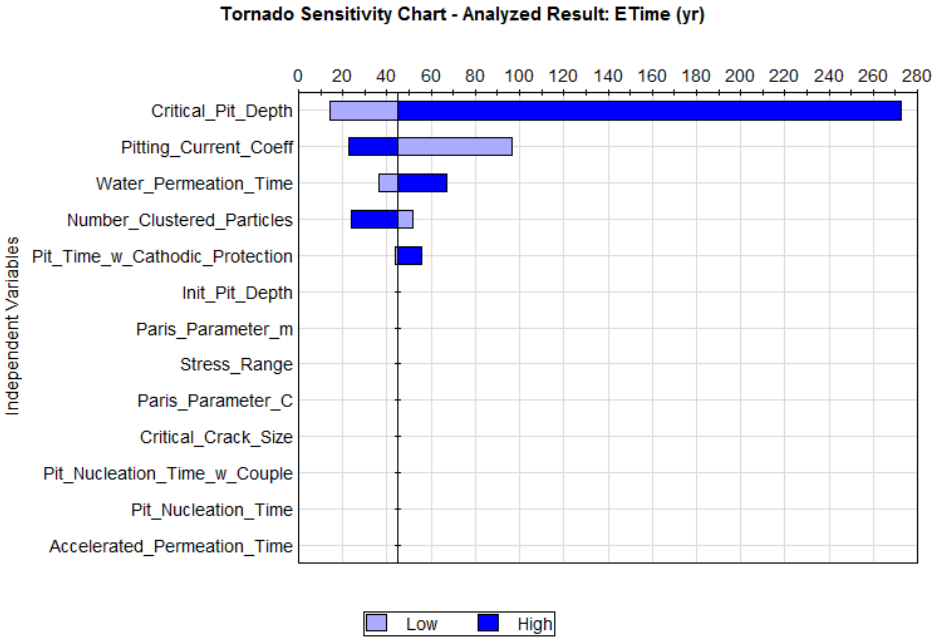

Figure 4-6: Failure Time Sensitivity Analysis Bar Chart

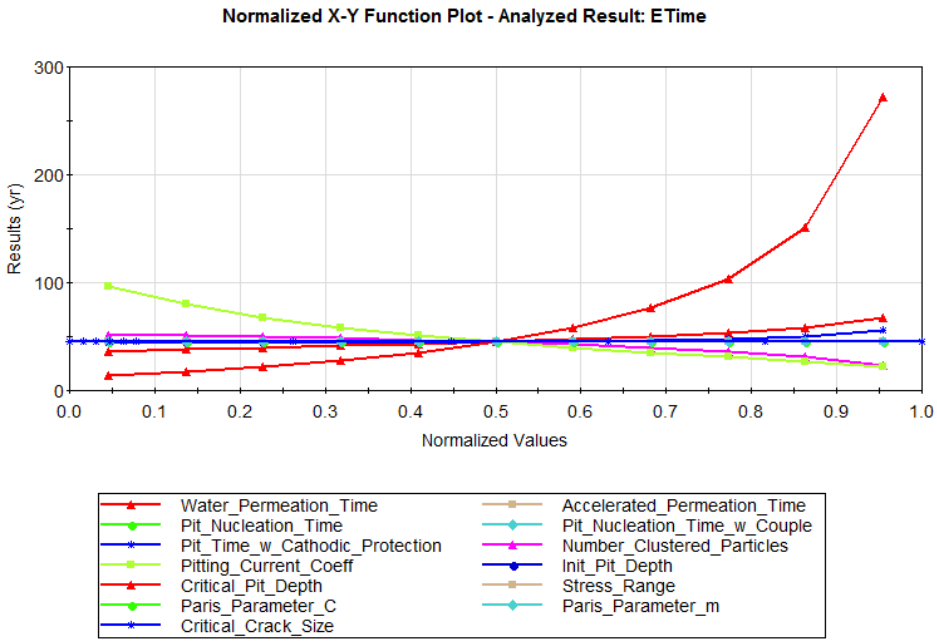

Figure 4-7: Failure Time Sensitivity Analysis X-Y Chart

In Figure 4-6, the results are arranged in descending order according to the range of shaft failure times produced. The light blue color indicates the result was produced using a value at the low end of the distribution while the dark blue color represents a high value result. The solid vertical line indicates the result using the central value for each variable. In Figure 4-7, the results are organized in a different manner. The y-axis represents the range of shaft failure times, while the x-axis represents normalized values for all the possible variables, since the units and ranges differ for each one [51].

From the diagrams, it can be seen that critical pit size has by far the largest effect on corrosion fatigue life. A value at the high end of the distribution can increase the time to failure to over 270 years, assuming mean values for all other random variables. Conversely, a value at the low end of the critical pit size distribution can reduce failure time to less than 15 years, a staggering 255 year range.

The pitting current coefficient has the second largest effect on corrosion fatigue life, with a value on the low end of its distribution increasing shaft life to almost 100 years.

The sensitivity of the results to the critical pit size is a key finding. As discussed

in Section 2.2, characterizing the localized corrosion morphology in terms of classical pitting can lead to misunderstanding. Pitting in materials that form a passive film (stainless steels) is characterized by pits with a large pit depth to diameter ratio. For carbon steels, the localized corrosion that is characterized as pitting exhibits a morphology with a much smaller depth/diameter ratio. Thus, as has been discussed earlier, the associated stress intensity factor for a carbon steel pit is likely to be smaller. However, if the localized corrosion is "focused" due to a galvanic couple where the cathode to anode area ratio is very large, as would be the case for the Alloy 625/carbon steel couple with compromised GRP, the associated evolution of the stress intensity factor would be expected to increase much faster than for the free corrosion case [12]. Thus, for the actual design, a large amount of uncertainty in this phase of the degradation process is expected.

4.6 Limitations and Uncertainty

It is important to point out once more that many of the simulated values possess a significant amount of uncertainty, which can be hard to quantify. While most of the model inputs are based off of experimental data, it is nearly impossible to replicate the exact environment and loading of full-scale shafts, impacting the predicted corrosion rate and corrosion fatigue life. Furthermore, most experiments are conducted using a compressed time scale, and Melchers points out that extrapolating the data and conclusions to actual systems can be "misleading" [13]. However, sometimes that data is the only information available, making their use necessary as long as the inherent variability is understood.

The mean times and standard deviations from the Monte Carlo simulation are shown in Table 4.6. Based on this data, there is still a large amount of uncertainty surrounding the corrosion fatigue life of a submarine propulsion shaft. Though the mean time of failure for the system is 21.55 years, a 5% to 95% confidence interval of shaft failure times spans almost 40 years, from 6.30 years to 46.18 years. That means that there is a 90% chance that shaft failure will occur somewhere in that range,

rendering the result's use in decision making processes difficult.

Condition	**Mean**	**Standard Deviation**
Time to First Water Ingress	4.78 yrs	3.76 yrs
Time to First Pit	8.31 yrs	4.40 yrs
Time to First Crack	21.52 yrs	12.84 yrs
Time to Failure	21.55 yrs	12.84 yrs

Table 4.6: Shaft Simulation Mean Times with Standard Deviation

THIS PAGE INTENTIONALLY LEFT BLANK

Chapter 5

Conclusions

The simulation results described in Chapter 4 paint a very bleak picture for 12-year shaft inspection intervals, assuming of course that the design matches the one described in this thesis. Though uncertainty surrounding the exact shaft failure time is still significant, the data suggests that some substantial design changes may be needed in order to prevent corrosion fatigue of the steel propulsion shaft.

5.1 Stopping the Corrosion Fatigue Chain

Corrosion fatigue is a sequential process. Consequently, if one of the initial steps in the process is prevented, then the risk of corrosion fatigue failure is essentially averted, or at least significantly reduced. Finding methods of interrupting this chain should remain a priority.

As expected, the void areas forward of the propeller, together with the stern tube and propeller bearings, were the first to fail a vast majority of the time. The long seawater permeation times modeled for the shaft span were a major factor in increasing its fatigue life. If increasing permeation times can have that sizable of an effect, then the focus should be to extend seawater ingress times for the remaining shaft components.

The Navy already uses coatings and seals in order to keep the shaft steel dry. While there is always room to improve upon these substances, especially at the sus-

ceptible interface points, other potential methods include paints, weld inlays, and even geometry changes to reduce stress concentrations at the discontinuities. The geometry changes would likely require significant engineering and manufacturing costs, but the benefits of reduced maintenance periods and maximized operation time would likely outweigh the increase in cost.

Even if the shaft becomes wetted, the proper use of cathodic protection systems or other methods of reducing corrosion current could stop or substantially hinder the corrosion chain before pits and cracks develop. In the updated model, the benefit of CP systems is represented with a 10% increase in corrosion pit nucleation time. Yet, the benefit may be significantly more, or less than that on real systems. Once the GRP at the interface between the Alloy 625 sleeve and carbon steel shaft has been compromised, the localized environment can evolve to be much more aggressive in terms of pH, and hence, corrosion rate. Cathodic protection will be much less effective in these areas.

However, the simulation results do not show an extreme sensitivity to the risk of galvanic corrosion at the bearing sleeve to shaft interface, even with an 80% chance of galvanic couple formation upon wetting. While the 10% reduction in pit nucleation time may be the cause, increasing the galvanic corrosion impact to equal a 25% reduction in pit nucleation time had little effect on overall shaft life, illustrated in Figure 5-1. In any case, once water ingress has occurred, the relationship between localized corrosion rate, pit nucleation time, crack initiation time and crack growth rate will determine remaining life.

5.2 Recommendations for Future Work

The goal of this thesis was to produce a second-generation model that could be used to provide useful shaft life predictions for a COLUMBIA-like ballistic missile submarine. Though the updated shaft life model incorporates additional components and features in an attempt to more realistically model the submarine propulsion shaft and reduce simulation uncertainty, the complexity of the system combined with the lack of open

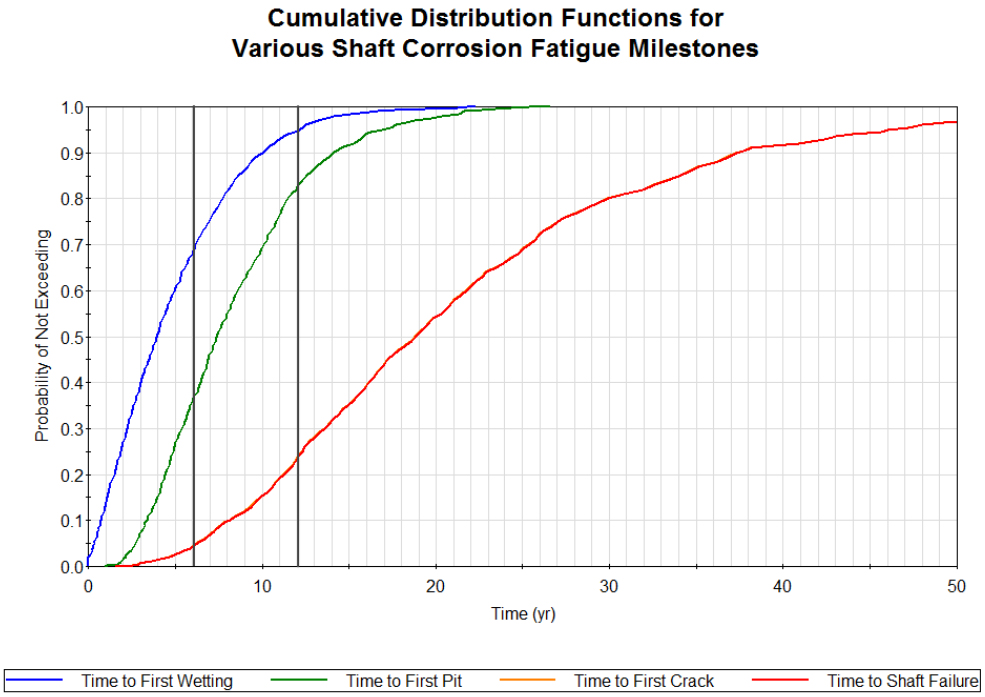

Figure 5-1: GoldSim Propulsion Shaft Failure Distribution with an Increased Galvanic Corrosion Effect

literature on the subject means that there are still many more ways to improve the model and the results.

5.2.1 Experimental Data

One such method is to obtain more relevant empirical data through experimentation, using the methods described by Jonart as a starting point [6]. It has already been shown how tailored and more representative data on submarine shafting can result in more accurate CP and galvanic corrosion predictions. However, tackling additional terms like pitting current coefficient I_{P0}, a term which Harlow and Wei described as having "the most uncertainty" of the random variables [39], would reduce some of the variation and produce more relevant results. A similar thought could be applied to pit nucleation time, especially since Shi and Mahadevan, from whom the distribution is referenced, focused primarily on aluminum alloys [19].

Based on the results of the sensitivity analysis in Section 4.5, another useful term

to focus on is critical pit size. By narrowing the range on its random variable distribution, the associated 255-year range in possible failure times should be reduced, similarly shrinking the 90% confidence interval for overall propulsion shaft life.

The next-generation model relies heavily on the work and data from experiments on similar materials in comparable environments. However, results using actual shaft material subjected to the stresses expected on an operational submarine would produce results with substantially less uncertainty, making predictions of fatigue life at any inspection interval much more useful.

Absent an ability to delay water ingress, accurate knowledge of the fatigue crack initiation and growth behavior will be key to evaluating time to failure and will thus dominate the inspection interval determination.

5.2.2 Data Availability

Another way to improve the model is to obtain more accurate target values using OHIO class submarine inspection reports. The updated shaft model was calibrated to the general target values of Table 4.1, but it can easily be modified to match more specific data points, based on data availability.

However, the characterization of defects on existing shaft inspection reports would likely have to be improved. As it stands now, future shaft models would have to conservatively assume that any evidence of corrosion is due to water ingress and that pitting, cracking, and failure would ultimately result. However, after talking to shaft experts at Portsmouth Naval Shipyard (PNSY), that is not always the case. Sometimes the observed corrosion was thought to be due to trapped moisture at the time of installation, only showing signs of corrosion once the coating was removed for inspection. This type of corrosion would still register as evidence of water ingress on inspection reports, artificially inflating the target values.

A similar issue is in play for pitting probabilities, with every pit assumed to be caused from the corrosion fatigue process. However, what looks like pitting could also result from other means, such as tool marks or metal samples during previous inspections. A better characterization of the pit at the time of inspection can allow

discrimination between the corrosion pits and these other non-corrosion pits.

The current inspection process is designed to simply identify areas that are suspect and thus in need of repair. Except for a limited number of inspection reports, a detailed characterization of the nature of a specific observation of corrosion is not usually performed. Thus, engineering judgement coupled with personal conversations with inspection teams have to be used — with attendant increase in uncertainty. A key takeaway from this research is that better characterizations of these indications would result in a significant improvement in the overall results with greatly reduced uncertainty.

5.2.3 Model Improvements

A final recommendation for future work would be to improve upon the probabilistic model itself. As mentioned in Chapter 3, the presence of cathodic protection systems or galvanic couples is incorporated into the model using a first order approximation. While more accurate experimental inputs would yield more accurate shaft life predictions, as mentioned in Section 5.2.1, the model could also be altered to determine actual corrosion current density and use actual protection current values. With a better understanding of the materials and environments involved, equilibrium potentials and current densities can be computed using an Evans diagram, yielding a more precise contribution for CP systems and galvanic couples alike.

Another more obvious area to improve the model would be to incorporate more shaft components, especially if the model is modified to represent other shafting systems outside of submarines. Items like mechanical couplings, sealing systems, and strut bearings on ships all exhibit different stresses and corrosion fatigue characteristics. Including them into the shaft life model would only improve the predictions.

5.3 The "Blue Sky" Solution

The second-generation model developed in this thesis assumes that the component configuration for the COLUMBIA class submarine will be similar to that for the

current OHIO class. Discussions with Navy shafting personnel indicate that the basic configuration in terms of geometry and materials of construction will be the same, but with additional efforts made to keep the shaft dry. While the assumption will be made that the time to water ingress will be improved, no estimate has been made as to by how much. However, achievement of a 12-year inspection interval will require that the probability of "failure" for this configuration be reduced to very low values.

A well-calibrated model using prototypic data that is updated using well-characterized inspection data will be essential to accurately define what the allowable inspection interval actually is. Thus, a fully calibrated Probabilistic Risk Assessment (PRA) that is based on an advanced model will be essential going forward. However, assuming that eventual water ingress will occur, a much better long-term effort should be placed on eliminating the pitting/cracking problem altogether. One way to do this is to fabricate the entire shaft with a corrosion resistant material. However, the cost for this fix may be extremely high and introduce other issues that greatly complicate the design. A better solution would be to modify the design such that the localized corrosion problem is eliminated but still allows the use of more traditional carbon steels.

The "Blue Sky" solution would be to design a system that extends the inspection interval to the life of the hull. Modern coating technologies, including weld overlay/inlay processing and cold spray technologies provide two, of many other options that may be considered. However, solving one problem — the galvanic couple as an example — may introduce other issues, such as high residual stresses, reduced fatigue crack initiation time, etc. that negate these benefits. It is thus essential that a systems approach be taken to the design of the shafting system. Such an approach, while requiring significant effort and time, would yield the ultimate solution to the problem of shaft degradation.

Appendix A

GoldSim Overview

GoldSim represents one of the many programs available to perform dynamic, probabilistic simulations. This appendix provides a brief overview of the GoldSim program, its capabilities, and what is needed to run the models described in this thesis.

According to its own User's Guide, GoldSim is a "highly graphical, object-oriented computer program for carrying out dynamic, probabilistic simulations" [51]. To perform these simulations, a model is created that represents the system in question, which can be from a wide range of applications such as business, science, and engineering. For the purposes of this thesis, the Reliability Module was extensively used in order to analyze the risk and probability of failure (i.e. reliability) of large complex systems, such as a submarine shaft. To propagate the uncertainty inherent in the system, GoldSim uses Monte Carlo simulation, where the model is run a large number of times with all simulations, or *realizations* equally likely. As a result, each realization represents a possible outcome of the system, and the uncertainty can be determined.

The power in GoldSim lies with its user-friendly graphical interface, where complex systems with multiple failure modes and elaborate interdependencies can still be easily modeled. Using a stochastic input, creating a triggered event, modeling an information delay, or viewing the cumulative distribution function of all the results is all done with the creation of a single element. Additionally, the creation of text boxes, shapes, and colors allows for easy documentation.

Once the model is created, running the simulation is as easy as setting the Monte Carlo parameters and clicking run. The program can automatically convert units, execute equations, and produce a range of outputs that can be used for analysis and presentation. An added benefit is that the licensed GoldSim software is not needed to view and execute a probabilistic GoldSim model. Third parties can download a GoldSim Player free from their website and run specialized program files created by a user with the full-licensed software.

For more information on GoldSim, refer to the GoldSim User's Guide, Reference [51].

Appendix B

List of Abbreviations and Symbols

Symbol	Description
CDF	Cumulative Distribution Function
CP	Cathodic Protection
CSE	Copper-Copper-Sulfate Reference Electrode
CV	Coefficient of Variation
FMEA	Failure Mode and Effects Analysis
GRP	Glass Reinforced Plastic
ICCP	Impressed Current Cathodic Protection
NACE	National Association of Corrosion Engineers
NNpH	Near Neutral pH
NOAA	National Oceanic and Atmospheric Administration
NPL	National Physical Laboratory
OPTEMPO	Operational Tempo
PDF	Probability Density Function
PNSY	Portsmouth Naval Shipyard
PRA	Probabilistic Risk Assessment
RPM	Revolutions Per Minute
RUL	Remaining Useful Life
SSBN	Ballistic Missile Submarine

Table B.1: List of Abbreviations

Symbol	Description
i_{corr}	Corrosion Current / Current Density
M	Molecular Weight
z	Valence
F	Faraday's Constant
ρ	Density of Steel
$\frac{\mathrm{d}}{\mathrm{d}t}$	Growth Rate
V	Volume
I_P	Pitting Current
n	Valence
I_{P0}	Pitting Current Coefficient
ϕ_k	Aspect Ratio
c_0	Initial Pit Size
ΔH	Activation Enthalpy
R	Universal Gas Constant
T	Absolute Temperature
t_{pg}	Time for Pit Growth from Initial to Critical Size
c_{ci}	Critical (Crack Initiation) Pit Size
K_t	Stress Concentration Factor
σ_a	Stress Amplitude
$\Delta\sigma$	Stress Range
$R = -1$	Fully Reversed Stress Ratio (R ratio)
ΔK_{th}	Threshold Stress Intensity Factor
k	Number of Constituent Particles
C	Paris Law Intercept Parameter
m	Paris Law Slope Parameter
ΔK	Stress Intensity Factor
α	Geometry Correction Factor
r_i	Shaft Inner Radius
r_o	Shaft Outer Radius
a	Shaft Crack Depth
t	Shaft Thickness
M_t	Moment
N_f	Number of Cycles until Failure
a_c	Critical Crack Size
a_i	Initial Crack Size

Table B.2: List of Symbols (in order of appearance)

Bibliography

[1] R. O'Rourke, "Navy Columbia (SSBN-826) Class Ballistic Missile Submarine Program: Background and Issues for Congress," *Congressional Research Service (CRS) Report*, Jan. 2018.

[2] S. K. Shoaib Nadeem, G. Giridhara, and H. K. Rangavittal, "A Review on the Design and Analysis of Composite Drive Shaft," *Materials Today: Proceedings*, vol. 5, pp. 2738–2741, Jan. 2018.

[3] M. Bhargava, "Emerging Technologies for Futuristic Submarines," *SP's Naval Forces*, no. 5, 2017.

[4] Q. Y. Wang, N. Kawagoishi, Q. Chen, and R. M. Pidaparti, "Probabilistic Modeling of Pitting Corrosion Fatigue Life," in *The Twelfth International Offshore and Polar Engineering Conference*, (Kitakyushu, Japan), May 2002.

[5] S.-X. Li and R. Akid, "Corrosion fatigue life prediction of a steel shaft material in seawater," *Engineering Failure Analysis*, vol. 34, pp. 324–334, Dec. 2013.

[6] D. E. Jonart, *Methods and Devices for Corrosion Fatigue Testing without Acceleration*. PhD, Massachusetts Institute of Technology, Cambridge, MA, June 2016.

[7] G. Vizentin, G. Vukelić, and M. Srok, "Common Failures of Ship Propulsion Shafts," *Scientific Journal of Maritime Research*, vol. 31, pp. 85–90, Dec. 2017.

[8] A. W. Peabody and R. L. Bianchetti, *Peabody's Control of Pipeline Corrosion*. Houston, TX: NACE International: The Corrosion Society, 2nd ed., 2001.

[9] D. A. Jones, *Principles and Prevention of Corrosion*. Englewood Cliffs, NJ: Prentice Hall, 2nd ed., 1996.

[10] P. P. Milella, *Fatigue and Corrosion in Metals [Electronic Resource]*. Milan: Springer-Verlag Italia, 2013.

[11] R. E. Melchers, "Probabilistic Model for Marine Corrosion of Steel for Structural Reliability Assessment," *Journal of Structural Engineering*, vol. 129, p. 1484, Nov. 2003.

[12] R. Ballinger, "Lecture Notes: Corrosion - The Environmental Degradation of Materials," *MIT Course 22.72J/3.54J*, 2015.

[13] R. E. Melchers, "Recent Progress in the Modeling of Corrosion of Structural Steel Immersed in Seawaters," *Journal of Infrastructure Systems*, vol. 12, p. 154, Sept. 2006.

[14] R. Pérez-Mora, T. Palin-Luc, C. Bathias, and P. C. Paris, "Very high cycle fatigue of a high strength steel under sea water corrosion: A strong corrosion and mechanical damage coupling," *International Journal of Fatigue*, vol. 74, pp. 156–165, May 2015.

[15] E. Arzaghi, R. Abbassi, V. Garaniya, J. Binns, C. Chin, N. Khakzad, and G. Reniers, "Developing a dynamic model for pitting and corrosion-fatigue damage of subsea pipelines," *Ocean Engineering*, vol. 150, pp. 391–396, Feb. 2018.

[16] M. Goto, "Corrosion fatigue behavior of a heat-treated carbon steel and its statistical characteristics," *Engineering Fracture Mechanics*, vol. 42, pp. 893–909, Jan. 1992.

[17] D. G. Harlow and R. P. Wei, "Probability Approach for Prediction of Corrosion and Corrosion Fatigue Life," *AIAA Journal*, vol. 32, pp. 2073–2079, Oct. 1994.

[18] M. T. Gudze and R. E. Melchers, "Operational based corrosion analysis in naval ships," *Corrosion Science*, vol. 50, pp. 3296–3307, Jan. 2008.

[19] P. Shi and S. Mahadevan, "Damage tolerance approach for probabilistic pitting corrosion fatigue life prediction," *Engineering Fracture Mechanics*, vol. 68, pp. 1493–1507, Jan. 2001.

[20] Special Metals Corporation, "Inconel Alloy 625 Technical Bulletin," Aug. 2013.

[21] National Corrosion Service, "Guide to Good Practice in Corrosion Control: Bimetallic Corrosion," 2000.

[22] J.-H. Kim, Y.-S. Kim, and J.-G. Kim, "Cathodic protection criteria of ship hull steel under flow condition in seawater," *Ocean Engineering*, vol. 115, pp. 149–158, Mar. 2016.

[23] Y. Kondo, "Prediction of Fatigue Crack Initiation Life Based on Pit Growth," *Corrosion*, vol. 45, pp. 7–11, Jan. 1989.

[24] D.-K. Kim, S. Muralidharan, T.-H. Ha, J.-H. Bae, Y.-C. Ha, H.-G. Lee, and J. D. Scantlebury, "Electrochemical studies on the alternating current corrosion of mild steel under cathodic protection condition in marine environments," *Electrochimica Acta*, vol. 51, pp. 5259–5267, Jan. 2006.

[25] "Standard Practice: Control of External Corrosion on Underground or Submerged Metallic Piping Systems," *NACE International*, no. SP0169-2013, 2013.

[26] F. Varela, M. Tan, and M. Forsyth, "Understanding the effectiveness of cathodic protection under disbonded coatings," *Electrochimica Acta*, vol. 186, pp. 377–390, Dec. 2015.

[27] T. Zhao, Z. Liu, C. Du, M. Sun, and X. Li, "Effects of cathodic polarization on corrosion fatigue life of E690 steel in simulated seawater," *International Journal of Fatigue*, vol. 110, pp. 105–114, May 2018.

[28] R. A. Gummow, "Cathodic protection criteria - A critical review of NACE Standard RP-01-69," *Materials Performance*, vol. 25, pp. 9–16, Sept. 1986.

[29] S. Lorenzi, T. Pastore, T. Bellezze, and R. Fratesi, "Cathodic protection modelling of a propeller shaft," *Corrosion Science*, vol. 108, pp. 36–46, July 2016.

[30] J. D. Garcia-Espinel, D. Castro-Fresno, P. Parbole Gayo, and F. Ballester-Muñoz, "Effects of sea water environment on glass fiber reinforced plastic materials used for marine civil engineering constructions," *Materials and Design*, vol. 66, pp. 46–50, Feb. 2015.

[31] H. Gu, "Behaviours of glass fibre/unsaturated polyester composites under seawater environment," *Materials and Design*, vol. 30, pp. 1337–1340, Jan. 2009.

[32] J. McCool, *Using the Weibull Distribution: Reliability, Modeling, and Inference*. Wiley Series in Probability and Statistics, Hoboken, NJ: John Wiley & Sons, 2012.

[33] J. Rajasankar and N. R. Iyer, "A probability-based model for growth of corrosion pits in aluminium alloys," *Engineering Fracture Mechanics*, vol. 73, pp. 553–570, Jan. 2006.

[34] B. Y. Fang, R. Eadie, W. X. Chen, and M. Elboujdaini, "Passivation/immersion method to grow pits in pipeline steel and a study of pit nucleation and growth resulting from the method," *Corrosion Engineering, Science and Technology*, vol. 44, pp. 32–42, Feb. 2009.

[35] D. G. Harlow and R. P. Wei, "A Probability Model for the Growth of Corrosion Pits in Aluminum Alloys Induced by Constituent Particles," *Engineering Fracture Mechanics*, vol. 59, pp. 305–325, Feb. 1998.

[36] A. Turnbull, L. N. McCartney, and S. Zhou, "A model to predict the evolution of pitting corrosion and the pit-to-crack transition incorporating statistically distributed input parameters," *Corrosion Science*, vol. 48, pp. 2084–2105, Jan. 2006.

[37] B. Y. Fang, R. L. Eadie, W. X. Chen, and M. Elboujdaini, "Pit to crack transition in X-52 pipeline steel in near neutral pH environment: Part 1 - formation of blunt cracks from pits under cyclic loading," *Corrosion Engineering, Science and Technology*, vol. 45, pp. 302–312, Aug. 2010.

[38] X.-g. Huang and J.-q. Xu, "3D analysis for pit evolution and pit-to-crack transition during corrosion fatigue," *Journal of Zhejiang University: Science A (Applied Physics and Engineering)*, vol. 14, p. 292, Apr. 2013.

[39] D. G. Harlow and R. P. Wei, "Probability modelling and statistical analysis of damage in the lower wing skins of two retired B-707 aircraft," *Fatigue & Fracture of Engineering Materials & Structures*, vol. 24, pp. 523–535, Aug. 2001.

[40] A. Carpinteri and M. Paggi, "A unified interpretation of the power laws in fatigue and the analytical correlations between cyclic properties of engineering materials," *International Journal of Fatigue*, vol. 31, pp. 1524–1531, Jan. 2009.

[41] S.-h. Xu and B. Qiu, "Experimental study on fatigue behavior of corroded steel," *Materials Science & Engineering A*, vol. 584, pp. 163–169, Nov. 2013.

[42] R. A. Locarnini, A. V. Mishonov, J. I. Antonov, T. P. Boyer, H. E. Garcia, O. K. Baranova, M. M. Zweng, C. R. Paver, J. R. Reagan, D. R. Johnson, M. Hamilton, and D. Seidov, *World Ocean Atlas 2013, Volume 1: Temperature*. Silver Spring, MD: NOAA Atlas NESDIS 73, 2013.

[43] N. Pugno, M. Ciavarella, P. Cornetti, and A. Carpinteri, "A generalized Paris' law for fatigue crack growth," *Journal of the Mechanics and Physics of Solids*, vol. 54, pp. 1333–1349, Jan. 2006.

[44] H. Tada, P. C. Paris, and G. R. Irwin, *The Stress Analysis of Cracks Handbook*. New York, NY: The American Society of Mechanical Engineers (ASME) Press, 3rd ed., 2000.

[45] A. Coppe, R. T. Haftka, N. H. Kim, and F.-G. Yuan, "Uncertainty Reduction of Damage Growth Properties Using Structural Health Monitoring," *Journal of Aircraft*, vol. 47, pp. 2030–2038, Nov. 2010.

[46] A. Coppe, M. J. Pais, R. T. Haftka, and N. H. Kim, "Using a Simple Crack Growth Model in Predicting Remaining Useful Life," *Journal of Aircraft*, vol. 49, pp. 1965–1973, Nov. 2012.

[47] D. An, J.-H. Choi, and N. H. Kim, "Identification of correlated damage parameters under noise and bias using Bayesian inference," *Structural Health Monitoring*, vol. 11, pp. 293–303, May 2012.

[48] S. Zhou and A. Turnbull, "Influence of pitting on the fatigue life of a turbine blade steel," *Fatigue & Fracture of Engineering Materials & Structures*, vol. 22, pp. 1083–1093, Dec. 1999.

[49] M. Mlikota, S. Staib, S. Schmauder, and Ž. Božić, "Numerical determination of Paris law constants for carbon steel using a two-scale model," in *Journal of Physics: Conference Series*, vol. 843, p. 012042, IOP Publishing, Jan. 2017. 843.

[50] M. Dehdab, Z. Yavari, M. Darijani, and A. Bargahi, "The inhibition of carbon-steel corrosion in seawater by streptomycin and tetracycline antibiotics: An experimental and theoretical study," *Desalination*, vol. 400, pp. 7–17, Dec. 2016.

[51] GoldSim Technology Group, "GoldSim User's Guide," July 2013.